J Cutan Pathol 2007: 34: 330–337
doi: 10.1111/j.1600-0560.2006.00614.x
Blackwell Munksgaard. Printed in Singapore

Journal of
Cutaneous Pathology

Granulomatous arteritis in cutaneous lesions of Churg–Strauss syndrome

Background: Although granulomatous arteritis is usually found in extracutaneous Churg–Strauss syndrome (CSS) lesions, the vasculitis in CSS cutaneous lesions typically shows small vessel vasculitis (leukocytoclastic vasculitis) without demonstrating the feature of granulomatous arteritis confirming the proper classification of CSS in the category of granulomatous vasculitis.
Methods: Four deep excisional biopsies were obtained from three untreated CSS patients who presented with livedo reticularis and subcutaneous nodules. Tissue blocks were recut and submitted for hematoxylin and eosin and elastic tissue staining to evaluate the histological features of the affected vessels. Immunostaining for histiocytes, lymphocytes, and neutrophils were performed on serial sections to confirm the cellular infiltration.
Results: In all specimens, subcutaneous granulomatous arteritis was observed. The unique histological feature distinct from other vasculitic disorders is characterized by marked infiltration of histiocytes and multinucleated giant cells in and around the disrupted subcutaneous arterial walls mixed with an eosinophilic infiltrate. In two specimens, granulomatous arteritis was found in the subsequent serial sections, not in the initial sections. The initial section may show extravascular granulomatous inflammation without evidence of vasculitis.
Conclusions: Granulomatous arteritis as identified in the extracutaneous lesions can also be found in subcutaneous CSS lesions presenting with livedo reticularis and/or subcutaneous nodules.

Chen K-R, Sakamoto M, Ikemoto K, Abe R, Shimizu H.
Granulomatous arteritis in cutaneous lesions of Churg–Strauss syndrome.
J Cutan Pathol 2007; 34: 330–337. © Blackwell Munksgaard 2006.

Ko-Ron Chen[1], Michiie Sakamoto[2], Kumiko Ikemoto[3], Riichiro Abe[4] and Hiroshi Shimizu[4]

[1]Department of Dermatology, Ogikubo Hospital, Tokyo,
[2]Department of Pathology, Keio University School of Medicine, Tokyo,
[3]Department of Internal Medicine, Ogikubo Hospital, Tokyo, and
[4]Department of Dermatology, Hokkaido University School of Medicine, Sapporo, Japan

Ko-Ron Chen, MD, PhD, Department of Dermatology, Saiseikai Central Hospital, 1-4-17 Mita, Minato-ku, Tokyo 108-0073, Japan
Tel: +81 3 3451 8211
Fax: +81 3 3451 6102
e-mail: chen@saichu.jp

Accepted for publication April 24, 2006

Churg–Strauss syndrome (CSS) is a rare clinicopathological entity, first reported by Churg and Strauss.[1] They noted significant clinical and histopathological differences between polyarteritis nodosa: marked eosinophilia in both tissues and peripheral blood, lung involvement, an allergic history of bronchial asthma, and specific histological features such as granulomas in both the vascular and extravascular lesions. Granulomatous arteritis of small- and medium-sized arteries, is an important and highly diagnostic finding in CSS, which accounts for CSS being categorized into the group of granulomatous vasculitides,[2–4] is observed in extracutaneous organs including the heart, gastrointestinal tract, lungs, kidneys, para-adrenal tissue, pancreas, spleen, liver, gallbladder, mesentery vessels, muscles, etc.[1,5–9]

Cutaneous vasculitis in CSS often shows features of necrotizing vasculitis in the dermal small vessels, arterioles, and venules[9–11] described as leukocytoclastic vasculitis,[10–13] which also can be found in several other vasculitic disorders.[11–13]

However, granulomatous arteritis in cutaneous lesions has never been clinically and histopathologically demonstrated in the English literature. We have thus far, encountered three CSS cases with histologically proven subcutaneous granulomatous arteritis and have outlined some of the pitfalls in diagnosis of granulomatous arteritis in cutaneous CSS lesions.

Materials and methods

Four deep excisional biopsies were obtained from three untreated CSS patients, who presented with subcutaneous nodules on the extremities in one patient and livedo reticularis on the lower legs in the remaining two patients.

A modifier of the American College of Rheumatology (ACR) criteria,[14] including (1) asthma, (2) eosinophilia >10% on differential white blood cell count, (3) mononeuropathy or polyneuropathy, (4) non-fixed pulmonary infiltrates on chest X-ray, (5) paranasal sinus abnormalities, and (6) a biopsy containing necrotizing vasculitis affecting small to medium vessels, instead of the less specific finding of extravascular eosinophil infiltration defined in ACR criteria,[14] is used for the diagnosis of CSS. All three cases met minimum requirements of at least four of the above criteria.

The four tissue blocks were recut and submitted for hematoxylin and eosin and elastic tissue staining in order to evaluate the histological features of the affected vessels and the adjacent areas on the corresponding serial sections.

To confirm the type of cellular infiltration, immunostaining for histiocytes, lymphocytes and neutrophils was performed on the corresponding serial sections. Granulomatous vasculitis is defined as a predominant infiltrate of histiocytes and/or multinucleated giant cells in and around the vessel wall, with evidence of vessel wall destruction such as fibrinoid necrosis. Medical details were reviewed for the clinical course and laboratory findings.

Case 1

A 79-year-old woman was referred to Department of Dermatology, Ogikubo Hospital in June 2003 with a 2-month history of painful skin lesions on her lower legs. She had initially presented with a dry cough with the chest X-ray revealing a transient right pulmonary peripheral patchy infiltrate and paresthesia of her lower extremities since November 2002.

Physical examination revealed widespread painful livedo reticularis on her lower legs (Fig. 1A) and footdrop in her left leg. Laboratory tests revealed mononeuritis multiplex of the lower legs and hypereosinophilia (2047/mm^3) with elevated myeloperoxidase-antineutrophil cytoplasmic antibody (MPO-ANCA) (74 EU) levels. Based on the clinical and laboratory findings, CSS was suspected, despite no history of asthma or allergic rhinitis.

Two deep excisional biopsies were taken from the areas of livedo reticularis on her lower left and right legs, respectively. The initial section showed subcutaneous extravascular and perivascular granulomatous inflammation mixed with eosinophilic infiltration without any evidence of vasculitis on the lower left leg biopsy specimen (Fig. 1B and 1C). In the lower right leg biopsy, arteritis resembling feature of cutaneous polyarteritis nodosa was observed in a subcutaneous artery characterized by predominant infiltrates of lymphocytes and histiocytes in and around the vessel wall (Fig. 2B) with intimal fibrinoid necrosis and disruption of the remaining internal elastic lamina (Fig. 2C). However, after serial sections were examined on both biopsy specimens, subcutaneous granulomatous arteritis presenting as a mixed histiocytic infiltrate with multinucleated giant cells in and around the disrupted arterial wall (Figs. 1E and 3A), was confirmed. The unique histiocytic infiltration around the involved artery was confirmed by immunostaining showing marked angiocentric CD68-positive staining (Fig. 3B) with CD45RO

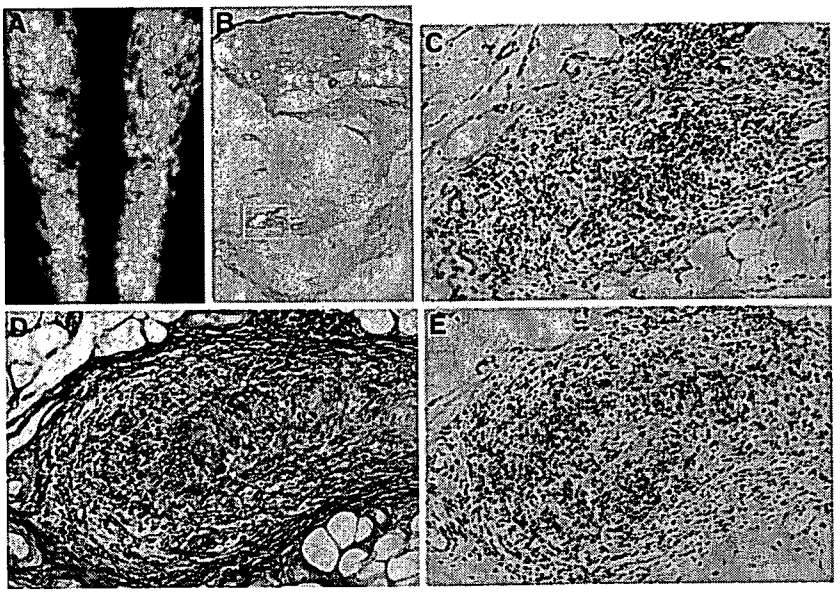

Fig. 1. (A) Livedo reticularis on the lower legs in case 1. (B) Histological features of the initial section from case 1 with livedo reticularis on the lower left leg that revealed perivascular inflammation in the deep subcutis (hematoxylin–eosin, ×5). (C) Higher magnification of (B) shows subcutaneous perivascular granulomatous inflammation without evidence of vasculitis (hematoxylin–eosin, ×50). (D) A further serial section shows perivascular granulomatous inflammation with marked multinucleated giant cells (arrows) in the infiltrate (elastica Van Gieson, ×50). (E) Evidence of subcutaneous granulomatous arteritis was found in the fifth serial section (hematoxylin–eosin, ×50).

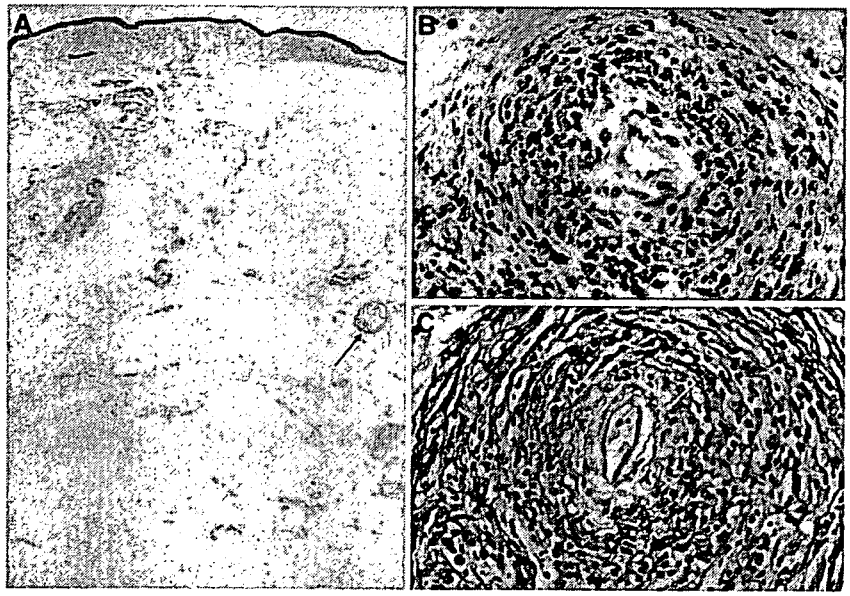

Fig. 2. (A) Histological features of the initial section from case 1 with livedo reticularis on the lower right leg showed arteritis resembling cutaneous polyarteritis nodosa in the deep subcutis (arrow) (hematoxylin–eosin, ×5). (B) Higher magnification of (A) shows intimal fibrinoid necrosis with mixed infiltrates of lymphocytes, neutrophils and histiocytes in and around the vessel wall (hematoxylin–eosin, ×50). (C) The remaining disrupted internal elastic lamina (arrow) with intimal fibrinoid necrosis of the same involved artery reveals features of necrotizing arteritis (elastica Van Gieson, ×50).

(UCHL-1)-positive staining at the periphery of the lesion (Fig. 3C) and almost negative staining for neutrophils (Fig. 3D).

A definite diagnosis of CSS was made based on the clinical and histological findings, despite no history of asthma. The patient was initially treated with prednisolone at 20 mg daily. Except for the persistent sensory disturbance, the footdrop and laboratory test abnormalities improved after the treatment and the livedo reticularis also gradually improved.

Case 2

A 47-year-old woman was referred to the Department of Dermatology, Keio University, School of Medicine, after a 2-month history of cutaneous lesions on her lower legs in September, 1987. She had a 3-year history of refractory asthma and a 3-month history of peripheral neuropathy in her lower legs, which gradually resulted in difficulty in moving.

Clinical and laboratory examinations showed livedo reticularis (Fig. 4A) with mononeuritis multiplex in her lower legs and hypereosinophilia (4752/$mm^{3)}$ with elevated IgE (5800 IU/ml)) levels and high titres of rheumatoid factor (5120 IU/ml).

A deep lesional biopsy (Fig. 4B) from the dorsal part of her left foot showed dermal perivascular eosinophilic infiltrates (Fig. 4C) with subcutaneous necrotizing granulomatous arteritis characterized by intimal fibrinoid necrosis and collections of multinucleated giant cells and histiocytes in and around the disrupted muscular vessel wall (Fig. 4D and 4E). CD68 immunostaining also showed a marked angiocentric

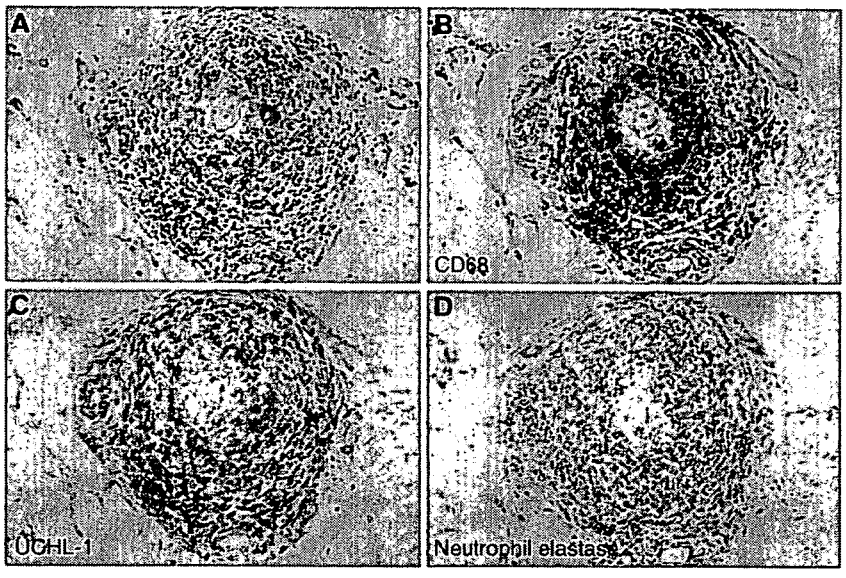

Fig. 3. (A) Granulomatous arteritis was identified in serial sections of Fig. 2 with marked infiltrates of histiocytes and multinucleated giant cells (arrow) in and around the vessel wall (hematoxylin–eosin, ×50). (B) Immunostaining shows marked angiocentric staining for CD68-positive cells presumed to be histiocytes. (C) Marked staining for T cells outside the histiocytic infiltration. (D) A lack of staining for neutrophils.

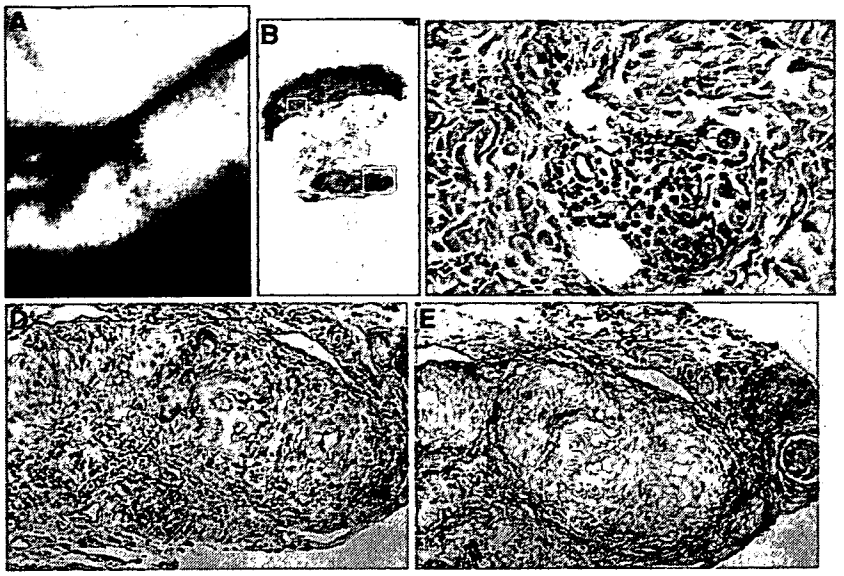

Fig. 4. (A) Livedo reticularis on the dorsum of the foot in case 2. (B) Histological features from the areas of livedo reticularis showed a vascular lesion in the deep subcutis (hematoxylin–eosin, ×5). (C) Higher magnification of (B) shows dermal perivascular eosinophilic infiltrate without evidence of vasculitis (hematoxylin–eosin, ×50). (D) Subcutaneous granulomatous arteritis with intimal fibrinoid necrosis surrounded by collections of histiocytes and multinucleated giant cells (arrow) with an eosinophilic infiltrate at the periphery (hematoxylin–eosin, ×50). (E) Disrupted internal elastic lamina (arrow) from the same affected vessel as seen in (D) (elastica Van Gieson, ×50).

histiocytic infiltrate surrounded by an adjacent CD45RO positive T cell infiltrate (data not shown) but no staining for neutrophils (data not shown).

Based on these unique pathological, clinical, and laboratory findings, a final diagnosis of CSS was made.

Except for the persistent sensory disturbance, all the clinical symptoms and abnormal laboratory findings immediately improved after initiation of the prednisolone treatment (30 mg daily). The patient is still followed up for bronchial asthma but has failed to develop systemic vasculitis over the past 17 years.

Case 3

A 51-year-old male was referred to the Department of Dermatology, Hokkaido University, School of Medicine, with a 2-month history of cutaneous lesions in August, 2002. He had a 22-year history of paranasal sinusitis, a 12-year history of asthma and a 1-year history of nephrosis.

Clinical examination revealed subcutaneous nodules on his forearms and lower legs. Pleural effusion was found and sputum smears showed numerous eosinophils together with marked hypereosinophilia (10,282/mm^3) consistent with a diagnosis of CSS.

A biopsy taken from subcutaneous nodules on the right forearm (Fig. 5A) showed subcutaneous necrotizing granulomatous arteritis with fibrinoid necrosis of blood vessel walls and a proliferative luminal obliteration (Fig. 5B). Granulomatous arteritis was characterized by predominant infiltrates of histiocytes and multinucleated giant cells in and around the vessel wall mixed with a marked eosinophilic infiltration (Fig. 5B). The angiocentric histiocytic infiltration was confirmed by CD68-positve staining (data not shown).

The patient was initially treated with 3 days of intravenous methylprednisolone 1000 mg/day, followed by prednisolone 60 mg daily, which was then gradually tapered. Abnormal laboratory findings and pleural effusion rapidly improved and the subcutaneous nodules were completely resolved 6 weeks after the treatment.

Discussion

Cutaneous lesions followed by peripheral neuropathy are the commonest features occurring in 50–80% of CSS patients reported in large-scale worldwide studies.[9,15–19] Various cutaneous manifestations can also be found in CSS including palpable purpura, petechiae, erythema multiforme-like lesions, urticarial wheals, vesicles, bullae, infarcts, ulceration, papules, plaques, cutaneous, and subcutaneous nodules and livedo reticularis.[8–10,15–21]

Histological features in CSS cutaneous lesions have been divided into three categories including: extravascular granulomas and leukocytoclastic vasculitis as the most common findings[10,15] and cutaneous polyarteritis nodosa-like[22] features, as a relatively rare finding.[10,15] Other histological patterns with tissue eosinophilia and non-specific granulomatous inflammation within the dermis or subcutis can be also found,[10] but none of these findings are crucial CSS diagnostic features.[10,23,24]

The granulomas in CSS are palisading granulomas rather than epithelioid granulomas found in sarcoidosis.

Granulomas may develop in the vascular areas as highlighted in this article and these granulomas are characterized by collection of histiocytes and multinucleated giant cells in and around the disrupted

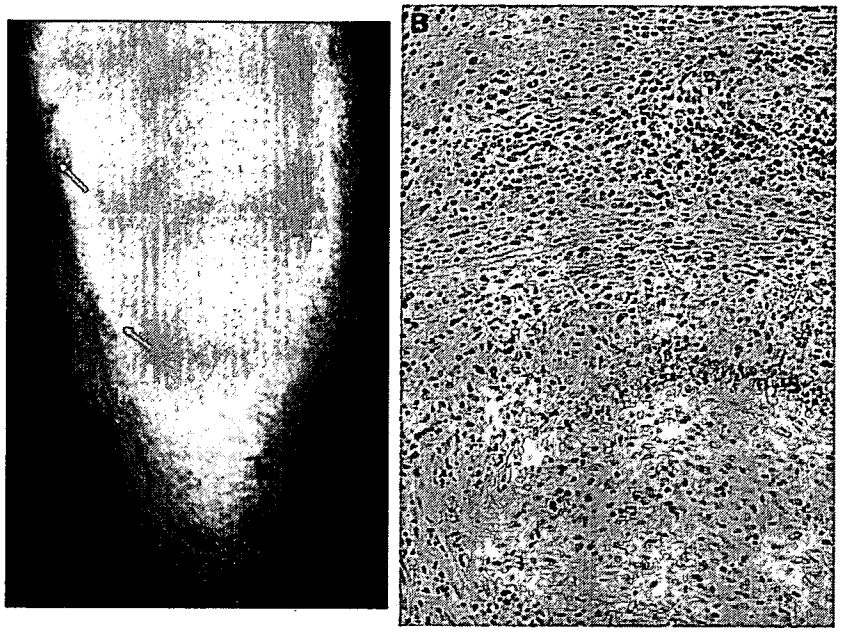

Fig. 5. (A) Subcutaneous nodules (arrows) on the forearm of case 3. (B) Histological features of the subcutaneous nodules in (A) shows subcutaneous granulomatous arteritis with proliferative luminal occlusion and fibrinoid necrosis surrounded by histiocytes in a palisading fashion (arrows) with a marked infiltrate of eosinophils at the periphery (hematoxylin-eosin, ×50).

artery in a palisading fashion (Figs 3A,B, 4D,E, and 5B). Granulomas may also develop in the extravascular areas either characterized by a basophilic central zone of necrobiotic collagen mixed with nuclear dust and neutrophils with a collection of palisading histiocytes at the periphery, which can be also found in other systemic diseases that clinically present as papules and/or nodules in elbow or knee joints (Winkelmann granuloma),[10,23,24] or characterized by the specific finding of so called CSS granuloma showing an eosinophilic central zone of necrobiotic collagen consisting of disintegrated eosinophils, surrounded by palisading histiocytes.[17,19]

As CSS is a systemic vasculitis involving all the organs including the skin, arteritis in the granulomatous stage (granulomatous arteritis) found in medium- to small-sized muscular arteries in the internal organs, should be possibly identified in the same caliber of muscular arteries in subcutis. Nevertheless, the original paper reported by Churg and Strauss stated that granulomatous arteritis was detected in the internal organs of their autopsy cases, but no areas of arteritis could be found in the skin lesions and no foci of granulomatous inflammation were observed within the vessel walls of cutaneous or subcutaneous nodules.[1,20]

The histological feature of arteritis in CSS reveals different patterns of cellular infiltrates during its inflammatory progression.[19] In the acute stage, the involved artery was found with a predominant eosinophilic infiltrate in and around the disrupted vessel wall consistent with features of eosinophilic arteritis (Fig. 6A); in the granulomatous stage, the involved artery was found with predominant infiltrates of histiocytes and multinucleated giant cells in and around the disrupted vessel wall (Fig. 6B); eventually in the final stage (healed stage), only fibrosis with a dearth of inflammatory cells or complete absence of inflammation is noted (Fig. 6C,D).[1,5–8,19]. Both these features of eosinophilic arteritis and granulomatous arteritis are different from those in polyarteritis nodosa that shows predominant infiltrates of neutrophils during the acute stage and predominant infiltrates of lymphocytes and histiocytes in healing stage (reparative stage).[19,22]

Arteritis in cutaneous CSS lesions of the type observed in cutaneous polyarteritis nodosa has rarely been recognized. Davis et al.[10] reported that only one patient with livedo reticularis out of 37 biopsy specimens from 29 CSS patients showed histological feature resembling cutaneous polyarteritis nodosa, which is clinically and histologically similar to our initial finding in case 1 (Fig. 2B,C). Crotty et al.[15] also reported arteritis resembling polyarteritis nodosa involving the muscular vessels of the deep dermis and subcutaneous fat in three cases out of 14 CSS patients. Two of the three patients revealed a mixed infiltrate of lymphocytes and histiocytes, that were consistent with our initial findings in case 1 (Fig. 2B,C) and the remaining case most likely showed features consistent with eosinophilic arteritis such as appreciable eosinophilic infiltration of the entire vessel wall. Nevertheless, further careful serial section investigations looking for granulomatous changes were not performed in both of these cases.

In addition to the relatively rare occurrence of arteritis in CSS skin lesions[10] the pitfalls listed in Table 1 may contribute to the rarity of granulomatous arteritis. Livedo reticularis is typically indicative

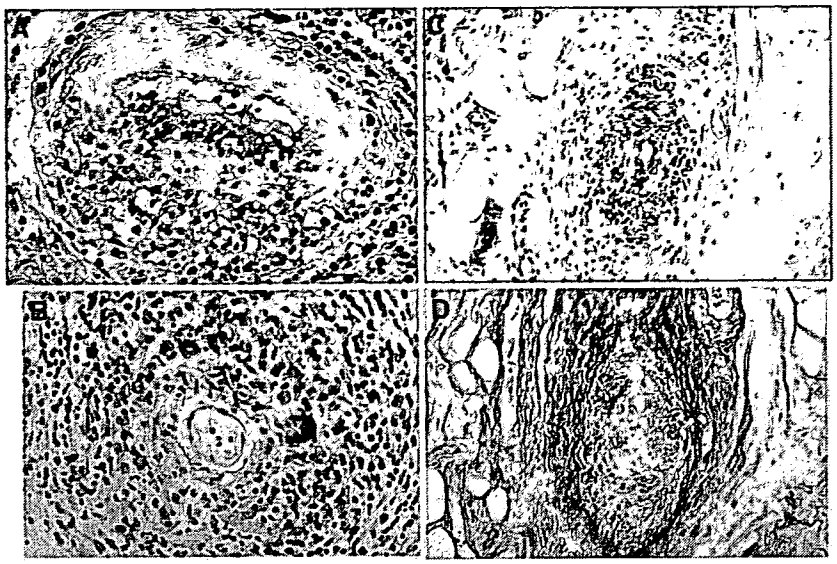

Fig. 6. Evolution of arteritis in CSS started as (A) the active stage with predominant infiltrate of eosinophils in and around the disrupted vessel wall suggestive of eosinophilic arteritis (cited from Chen KR et al. J Dermatol 1992; 19: 40–47), followed by (B) the granulomatous stage (case 1), and eventually progressed into (C) the healed stage (case 1) with intimal proliferation and marked disruption of the internal elastic lamina (D, arrow). There is a total absence of inflammation.

of a deep-seated occlusive arterial disease and any patients who present with livedo reticularis should have a biopsy that extends into the subcutis for adequate visualization of potentially diseased subcutaneous structures, as was demonstrated in our cases.

Without investigating multiple serial sections, one might only detect peri- or extravascular granulomatous inflammation without evidence of vasculitis (Fig. 7) as appeared in the original article by Churg and Strauss[1] and Strauss et al.[20] One of our initial sections in case 1 also showed perivascular granulomatous inflammation without evidence of vasculitis (Fig. 1C).

Other reasons that account for the rarity of granulomatous arteritis include taking the skin biopsy at an inappropriate time to sample the granulomatous stage during its inflammatory progression stage, or biopsying while the patient is already undergoing treatment with systemic steroids, as the inflammatory progression of the affected artery may shorten the granulomatous stage under these conditions and speed the progress into the healed stage earlier.[25]

The differential diagnosis of subcutaneous granulomatous arteritis encompasses temporal arteritis[26] (also termed giant cell arteritis), Wegener's granulomatosis, giant cell aortitis, necrotizing sarcoidosis, polyarteritis nodosa in the reparative stage and nodular vasculitis.[27] In temporal arteritis, the affected vessels include small- and medium-sized arteries with a predilection to involve the cranial vasculature and only on rare occasions can part of the morphologic expression of temporal arteritis be giant cell aortitis. Such cases are unaccompanied by significant extravascular inflammation including in the context of foci of palisading granulomas and/or significant tissue eosinophilia. Wegener's granulomatosis, is a small vessel vasculitic syndrome and hence, while there may be a granulomatous arteritis, the caliber of artery affected is relatively small as opposed to the potentially larger arteries with macroscopic polyarteritis nodosa-like features encountered in some cases of CSS. In necrotizing sarcoidosis, the granulomas have an epithelioid cohesive quality which is not a finding observed in either Wegener's granulomatosis or CSS. Giant cell aortitis may be associated with temporal arteritis, Reiter's disease and rheumatic fever and is the only true large vessel elastic artery containing arteritis. While CSS can involve medium-sized vessels, there is no involvement of the vessels that is anatomically categorized as large elastic containing arteries. During the reparative stage of polyarteritis nodosa, mixed infiltrates of histiocytes, lymphocytes, and eosinophils can be found in and around the involved subcutaneous artery, which is different from the unique features of subcutaneous granulomatous arteritis in CSS that predominantly exhibit

Table 1. Common pitfalls causing a failure to detect granulomatous arteritis in cutaneous CSS lesions

1. A skin biopsy was not performed over areas of livedo reticularis, a rare but significant vasculitic manifestation of CSS.
2. A suitable deep excisional biopsy was not conducted to obtain vasculitic lesions in subcutis.
3. Confirmation of the granulomatous arteritis in multiple, serial sections was not adequately performed.
4. The biopsy was taken after the start of treatment. Cases treated with systemic steroids may shorten the granulomatous stage and speed up the progression into the healed stage.
5. The biopsy was not taken at the right time to detect the granulomatous stage.

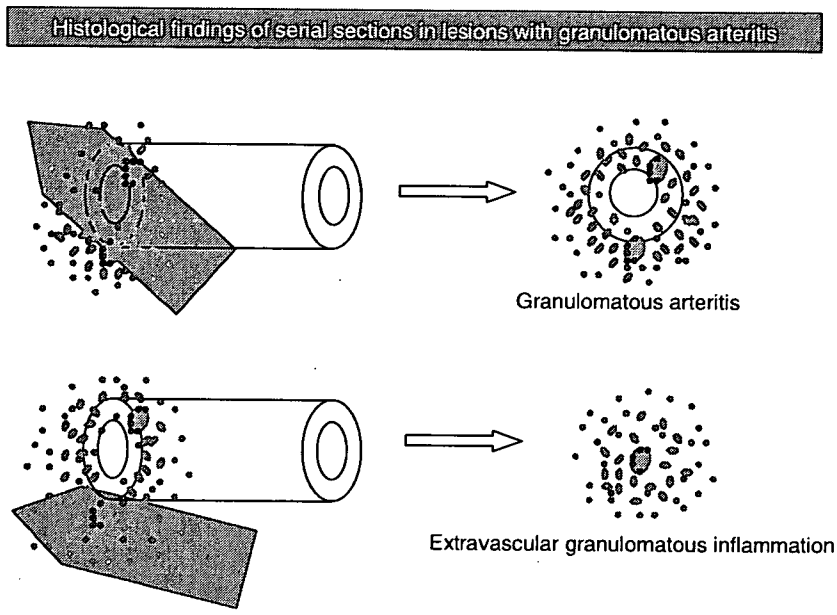

Fig. 7. Schema of the generalized histological findings after observing serial sections in granulomatous arteritis. Side sections of the main lesions reveal extravascular granulomatous inflammation.

infiltrates of histiocytes and palisading multinucleated giants cells around the disrupted artery. In nodular vasculitis/erythema induratum Bazin, feature of granulomatous vasculitis can be found in the same caliber of vessels in the subcutis, however, small- to medium-sized muscular veins rather than the arteries are the most often affected vessels.[27] Moreover, the lobular panniculitis with tuberculoid granulomas characterized by histiocytes and giant cells surrounding the caseous fat necrosis in nodular vasculitis is distinct from the focal panniculitis around the affected arteries in CSS.

CSS is a systemic vasculitic disease with tissue eosinophilia which may result in acute fatal heart failure during its clinical course.[7,9,19] Although the diagnosis of CSS can be difficult, timely treatment may prevent serious morbidity or death. As granulomatous arteritis in cutaneous lesions is a significant diagnostic feature of CSS, dermatologists will continue to play a key role in establishing a definite, early diagnosis in suspected CSS patients exhibiting livedo reticularis together with subcutaneous nodules if the aforementioned suitable, deep excisional biopsy and careful, multiple serial section histological examinations are conducted.

References

1. Churg J, Strauss L. Allergic granulomatosis, allergic angiitis, and periarteritis nodosa. Am J Pathol 1951; 27: 277.
2. Marquez J, Flores D, Candia L, Espinoza LR. Granulomatous vasculitis. Curr Rheumatol Report 2003; 5: 128.
3. Hammar SP. Granulomatous vasculitis. Semin Respir Infect 1995; 10: 107.
4. Jorizzo JL. Classification of vasculitis. J Invest Dermatol 1993; 100: 106S.
5. Lie JT. The classification of vasculitis and a reappraisal of allergic granulomatosis and angiitis. Mt Sinai J Med 1986; 53: 429.
6. Koss MN, Antonovych T, Hochholzer L. Allergic granulomatosis (Churg–Strauss syndrome): pulmonary and renal morphologic findings. Am J Surg Pathol 1981; 5: 21.
7. Sasaki A, Hasegawa M, Nakazato Y, Ishida Y, Saito S. Allergic granulomatosis and angiitis (Churg–Strauss syndrome): report of an autopsy case in a nonasthmatic patient. Acta Pathol Jpn 1988; 38: 781.
8. Reid AJC, Harrison BDW, Watts RA, Watkin SW, McCann BG, Scott DGI. Churg–Strauss syndrome in a district hospital. Q J Med 1998; 91: 219.
9. Guillevin L, Cohen P, Gayraud M, et al. Churg–Strauss syndrome, clinical study and long-term follow-up of 96 patients. Medicine (Baltimore) 1999; 78: 26.
10. Davis MDP, Daoud MS, McEvoy MT, Su WPD. Cutaneous manifestations of Churg–Strauss syndrome: a clinicopathologic correlation. J Am Acad Dermatol 1997; 37: 199.
11. Gibson LE. Cutaneous vasculitis: approach to diagnosis and systemic associations. Mayo Clin Proc 1990; 65: 221.
12. Barnhill RL, Busam KJ, Nousari CH, et al. Vascular diseases. In Elder DE, ed. Lever's histopathology of the skin. Philadelphia: Lippincott Williams & Wilkins, 2005; 215.
13. Ackerman AB, ed. Vasculitis. In Histologic diagnosis of inflammatory skin diseases: an algorithmic method based on pattern analysis, 2nd ed. Baltimore: Williams & Wilkins Co., 1997; 128.
14. Masi AT, Hunder GG, Lie JT, et al. The American College of Rheumatology 1990 criteria for the classification of Churg–Strauss syndrome (allergic granulomatosis and angiiitis). Arthritis Rheum 1990; 33: 1094.
15. Crotty CP, DeRemee RA, Winkelmann RK. Cutaneous clinicopathologic correlation of allergic granulomatosis. J Am Acad Dermatol 1981; 5: 571.
16. Nagasawa T, Yoshida M. Clinical features of allergic granulomatosis angitis in Japan and the propose of guideline for diagnosis of this disease. Jpn J Intern Med 1989; 78: 352 (abstract in English).
17. Shwartz RA, Churg J. Churg–Strauss syndrome. Br J Dermatol 1992; 127: 199.

18. Solans R, Bosch JA, Perez-Bocanegra C, et al. Churg–Strauss syndrome: outcome and long-term follow-up of 32 patients. Rheumatology 2001; 40: 763.
19. Lanham JG, Churg J. Churg–Strauss syndrome. In Churg A, Churg J, eds. Systemic vasculitides. New York: Igaku-Shoin Medical Publishers, 1991; 101.
20. Strauss L, Churg J, Zak FG. Cutaneous lesions of allergic granulomatosis: a histopathologic study. J Invest Dermatol 1951; 17: 349.
21. Chen KR, Ohata Y, Sakurai M, Nakayama H. Churg–Strauss syndrome: report of a case without pre-existing asthma. J Dermatol 1992; 19: 40.
22. Chen KR. Cutaneous polyarteritis nodosa. a clinical and pathological study of 20 cases. J Dermatol 1989; 16: 429.
23. Dicken CH, Winkelmann RK. The Churg–Strauss granuloma: cutaneous, necrotizing, palisading granuloma in vasculitis syndrome. Arch Pathol Lab Med 1978; 102: 576.
24. Finan MC, Winkelmann RK. Cutaneous extravascular necrotizing granuloma (Churg–Strauss granuloma) and systemic disease. a review of 27 cases. Medicine (Baltimore) 1983; 62: 142.
25. Baggenstoss AH, Shick RM, Polley HF. The effect of cortisone on the lesions of periarteritis nodosa. Am J Pathol 1951; 27: 537.
26. Mambo NC. Temporal (granulomatous) arteritis: a histopathological study of 32 cases. Histopathology 1979; 3: 209.
27. Sánchez Yus E. About the histopathology of erythema induratum-nodular vasculitis. Am J Dermatopathol 1999; 21: 301.

Circ J 2007; **71:** 132–137

Sustained-Release Erythropoietin Ameliorates Cardiac Function in Infarcted Rat-Heart Without Inducing Polycythemia

Xue Lin, MD; Masatoshi Fujita, MD*; Naoki Kanemitsu, MD; Yu Kimura, MD**; Keiichi Tambara, MD; Goditha U. Premaratne, MD; Atsushi Nagasawa, MD; Tadashi Ikeda, MD; Yasuhiko Tabata, PhD**; Masashi Komeda, MD

Background The usefulness of sustained-release erythropoietin for improving left ventricular (LV) function without polycythemia was evaluated in a rat chronic myocardial infarction model.

Methods and Results Four weeks after left coronary artery ligation, 50 Sprague-Dawley rats were assigned to 5 groups (n=10, each). Control group had a gelatin sheet (20×20 mm) containing saline applied to the infarct area, whereas the 4 treatment groups had gelatin sheets incorporating erythropoietin 0.1 U, 1 U, 10 U and 100 U, respectively. Endpoint measurements performed at 8 weeks after the coronary ligation revealed that the fractional area change was larger for erythropoietin 1 U and 10 U than in the other 3 groups. The LV end-systolic elastance and the time constant of isovolumic relaxation were better for erythropoietin 1 U and 10 U than in the other 3 groups. The density of vessels larger than 50 μm in diameter was the highest in the erythropoietin 1 U group. The number of red blood cells was significantly increased in groups receiving erythropoietin 10 U and 100 U.

Conclusions Gelatin hydrogel sheets incorporating 1 U erythropoietin improved LV function without inducing polycythemia in a rat chronic myocardial infarction model. (*Circ J* 2007; **71:** 132–137)

Key Words: Angiogenesis; Chronic myocardial infarction; Erythropoietin; Sustained-release; Ventricular remodeling

Recent advances in coronary reperfusion strategies and pharmacological management have resulted in an increasing number of survivors of acute myocardial infarction (AMI) who have a higher risk of developing left ventricular (LV) remodeling and chronic heart failure. Although therapeutic approaches aimed at delivering blood flow to the myocardium at risk are needed to improve cardiac function and prevent progression of LV remodeling, some patients have no revascularization options because of the diffuse nature of their coronary artery lesions. In such patients, therapeutic angiogenesis is being explored as an alternative strategy for providing significant blood flow to the akinetic myocardial tissue. Although initial uncontrolled clinical studies of therapeutic angiogenesis have generated a great deal of hope, the effectiveness of angiogenic growth factor has not been confirmed by subsequent randomized trials[1,2]

As a result, delivery strategies to achieve clinically significant angiogenic responses with sustained-release (SR) angiogenic growth factors are being explored[3–5] Recently, we developed a biodegradable gelatin hydrogel sheet incorporating basic fibroblast growth factor (bFGF), which enabled the bFGF to be released at the site of action for a sufficient time period[6,7]

Several recent studies have demonstrated that erythropoietin (EPO) has protective effects against ischemic injury in the brain[8] spinal cord[9] retina[10,11] kidney[12] and most recently, in the myocardium[13–17] EPO treatment has been reported to improve cardiac function in a post-infarction heart failure model[18–20] However, systemic treatment with a large dose of EPO is accompanied by polycythemia as an endogenous function of EPO, which may predispose to thromboembolic complications[15,18]

Thus, in the present study, we aimed to develop a biodegradable gelatin hydrogel sheet incorporating EPO and to determine the appropriate dose of EPO for improving LV function without inducing polycythemia in a rat chronic myocardial infarction (MI) model.

Methods

Male Sprague-Dawley rats were used in this study. All experimental procedures were performed in accordance with the guidelines for Animal Experiments of Kyoto University, which conforms to the law of "Guide for the Care and Use of Laboratory Animals" in Japan and conforms to the "Guide for the Care and Use of Laboratory Animals" published by the US National Institutes of Health (NIH Publication No. 85-23, revised 1996).

Preparation of Gelatin Hydrogel Sheets Incorporating EPO

Gelatin was prepared through an acid process of pig skin type I collagen and kindly supplied by Nitta Gelatin, Osaka, Japan. Gelatin hydrogel sheets were made using the pre-

(Received August 1, 2006; revised manuscript received September 19, 2006; accepted October 13, 2006)

*Department of Cardiovascular Surgery, Graduate School of Medicine, *School of Health Sciences, Faculty of Medicine and **Department of Biomaterials, Field of Tissue Engineering, Institute for Frontier Medical Sciences, Kyoto University, Kyoto, Japan*

Mailing address: Masashi Komeda, MD, Professor and Chairman, Department of Cardiovascular Surgery, Graduate School of Medicine, Kyoto University, 54 Kawahara-cho, Shogoin, Sakyo-ku, Kyoto 606-8507, Japan. E-mail: komelab@kuhp.kyoto-u.ac.jp

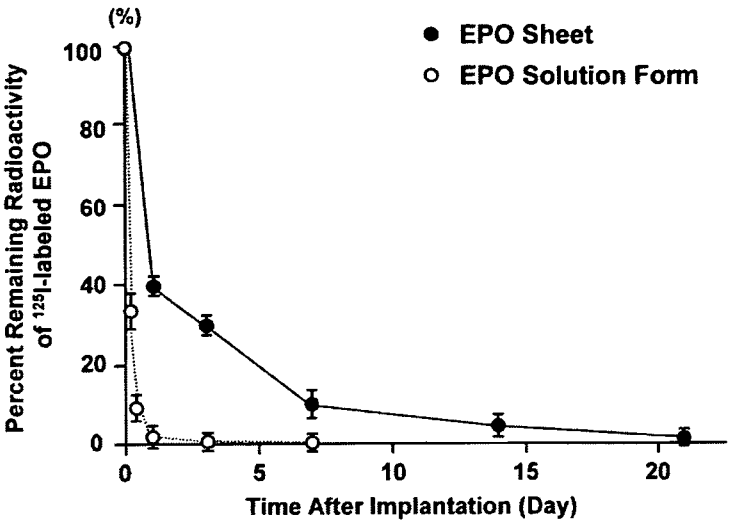

Fig 1. Time course of residual radioactivity at the site of injection with EPO solution and implantation with EPO incorporating gelatin hydrogel sheets. Error bars show SEM. The number of rats for each time point was 3. EPO, erythropoietin.

viously described process[21,22] Sheets were freeze-dried and cut in a rectangular shape for impregnation with phosphate buffered saline containing EPO (3,000 U in 0.5 ml; Sigma, Tokyo, Japan) at room temperature for 3 h. The prepared EPO-incorporating gelatin hydrogel sheets were used immediately after preparation.

In Vivo Evaluation of EPO Release and Gelatin Hydrogel Sheet Degradation

Gelatin hydrogels incorporating ^{125}I-labeled EPO were implanted subcutaneously into the dorsum of the mice, and 100 μl of subcutaneously injected aqueous solution of ^{125}I-labeled EPO was used as a control. The mice were killed at various intervals, and the skin around the EPO-implant or injection site was cut into strips. The fascia was thoroughly wiped with filter paper and the remaining radioactivity of the gelatin hydrogel, excised skin, and filter paper was measured on a gamma counter (ARC-301B; Aloka Co Ltd, Tokyo, Japan) to evaluate the time profile of in vivo degradation of the gelatin hydrogels.

Chronic MI Model

MI was created in rats weighing 250–290 g by ligating the proximal left anterior descending (LAD) coronary artery through a left thoracotomy, as described in our previous reports[23–27] Four weeks after the LAD ligation, infarction size and cardiac function were evaluated by means of echocardiography and cardiac catheterization, as described below.

Experimental Groups Four weeks after the coronary artery ligation, 50 rats with moderate-sized MI were assigned to 5 groups (each group, n=10). Group I, which had a saline-incorporated gelatin hydrogel sheet, served as the controls, and groups 2–5 had gelatin hydrogel sheets incorporating 0.1 U, 1 U, 10 U and 100 U of EPO, respectively. In each group, the rectangular gelatin hydrogel sheet was stabilized to the LV wall with 6-0 polypropylene sutures to cover the area of MI completely[23]

Echocardiography

Echocardiography assessment was performed according to the method previously described[23–27] In brief, LV dimension and function were assessed just before treatment, and followed up 2 and 4 weeks later. Images were recorded using a 10–12 MHz phased array transducer (Model 21380A with HP SONOS 5500 imaging system, Agilent Technologies, Andover, MA, USA). LV end-diastolic and end-systolic dimensions (LVDd and LVDs, respectively) were measured with M-mode tracings from the short-axis view of the LV at the papillary muscle level. Fractional area change (FAC) and the percentage of akinetic endocardial length to the whole LV endocardial circumference (AL) were also calculated from the same short-axis view. All measurements were performed in a blind fashion according to the American Society of Echocardiology, and averaged over 3 consecutive cardiac cycles.

Cardiac Catheterization

After the final echocardiographic evaluation, the rats underwent cardiac catheterization for more precise assessment of global LV function as described previously[23,25] In brief, under general anesthesia, a 2F micromanometer-tipped catheter (Millar Instruments Inc, Houston, TX, USA) was inserted via the right carotid artery into the LV, and a 3F occlusion balloon catheter through the right femoral vein into the inferior vena cava. LV pressure and its first time-derivative (dp/dt) were continuously monitored using a multiple recording system. The LV end-systolic volume was calculated from the M-mode echocardiograms by the cube formula. During the inferior vena cava occlusion with the balloon, pressure waveforms and M-mode tracings were simultaneously recorded, and the end-systolic elastance (Ees) and the time constant of isovolumic relaxation (Tau) were derived from the recorded data. In calculating Ees, the end-systolic pressure–volume points obtained from echocardiography and cardiac catheterization were subjected to least squared linear regression. All data were acquired under stable conditions.

Analysis of Vascular Density

After the final hemodynamic assessment, all rats were killed for the histological study. The specimens were paraffin-embedded, and the whole hearts were sectioned in 3 μm thickness at 100 μm intervals along the short axis. In the peri-MI area, the number of vessels was counted in each heart using immunohistochemistry for von Willebrand factor (U0034; Dako A/S, Glostrup, Denmark). The vessels per 1 mm^2 in the pertinent zone were counted in 3 randomly chosen fields per slide in a blind manner and averaged for statistical analysis.

Table 1 Echocardiographic Data

	Control	EPO			
		0.1 U	1 U	10 U	100 U
LVDd (cm)					
Before	1.06±0.06	1.09±0.06	1.07±0.05	1.08±0.07	1.07±0.08
After	1.12±0.02*	1.12±0.04	1.01±0.02*,†,‡,¶	1.04±0.03†,‡,¶	1.10±0.02
LVDs (cm)					
Before	0.87±0.07	0.88±0.06	0.86±0.06	0.87±0.09	0.86±0.05
After	0.94±0.02*	0.94±0.04*	0.81±0.02*,†,‡,¶	0.84±0.04†,‡,¶	0.88±0.02
FAC (%)					
Before	33.7±2.6	34.0±4.0	33.8±4.3	33.4±3.9	33.2±2.3
After	25.9±0.9*	29.0±2.1*	39.0±1.5*,†,‡,¶	35.9±2.1†,‡,¶	28.3±1.2
AL (%)					
Before	25.7±3.3	27.0±2.5	25.3±3.0	26.6±3.1	26.1±2.5
After	30.9±1.5*	28.6±2.3	21.0±0.6*,†,‡,¶	23.6±3.1*,†,‡,¶	27.1±1.8

Values are mean±SEM.
EPO, erythropoietin; LVDd, left ventricular end-diastolic dimension; LVDs, left ventricular end-systolic dimension; FAC, fractional area change; AL, percentage of akinetic endocardial length to the whole left ventricular endocardial circumference.
**p<0.05 vs values before treatment in the same group. †p<0.05 vs control; ‡p<0.05 vs EPO 0.1 U; ¶p<0.05 vs EPO 100 U.*

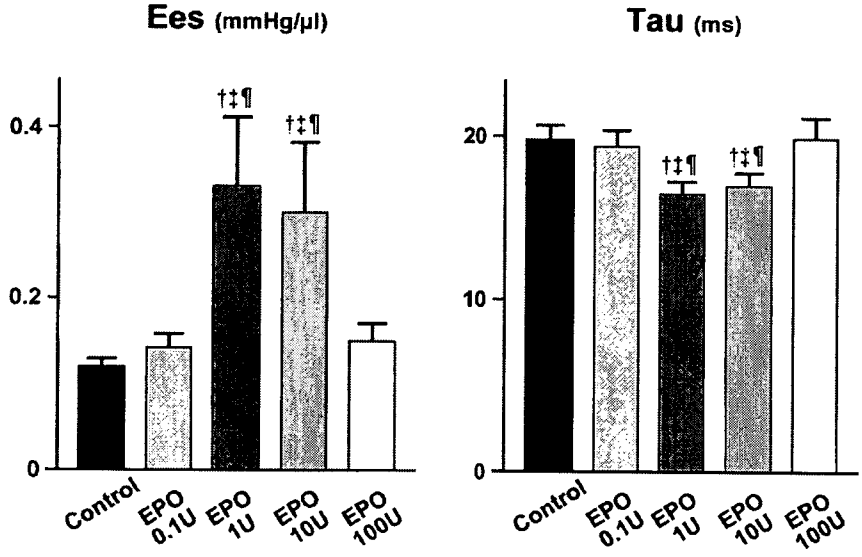

Fig 2. Data on cardiac catheterization. Error bars show SEM. Ees, end-systolic elastance; Tau, time constant of isovolumic relaxation; EPO, erythropoietin. †p<0.05 vs control, ‡p< 0.05 vs EPO 0.1 U, ¶p<0.05 vs EPO 100 U.

Measurement of Red Blood Cells (RBC)

Blood samples were obtained from a peripheral tail vein of sedated rats at 0, 2, and 4 weeks after the treatment. Samples were analyzed using a Celltac (Model MEK-6358, NIHON KODEN, Japan).

Data Analysis

All data are expressed as the mean ± standard error of the mean. Comparisons of echocardiographic data and the number of RBC among the groups were performed by 2-way repeated measures analysis of variance (ANOVA) including time, group, and group-by-time interaction terms. Comparisons of cardiac catheterization data and vascular density among the groups were conducted by one-way factorial ANOVA. All statistical analyses were performed using computer software (StatView for Windows version 5.0, SAS Institute Inc, Cary, NC, USA). A p-value <0.05 was considered statistically significant.

Results

Both the mortality after coronary artery ligation and the size of the MI were similar to our previous reports[26,27]

EPO Concentration by Gelatin Sheet Treatment

Fig 1 depicts the time course of remaining radioactivity of ^{125}I-labeled EPO after subcutaneous injection of EPO solution or subcutaneous implantation of gelatin hydrogels sheet incorporating EPO. More than 95% of the EPO injected as solution was cleared from the injected site within 1 day, whereas there was a prolonged release of EPO from the hydrogel at the site of implantation.

Echocardiography

There were no significant differences among the 5 groups in any data for cardiac function at 4 weeks after coronary artery ligation (Table 1). In the analyses of LVDd and LVDs, group and time effects and group-by-time interactions were strongly recognized. At 4 weeks after each treatment, LVDd in the groups with EPO 1 U and 10 U was significantly smaller than in the control group and the groups with EPO 0.1 U and 100 U. The groups with EPO 1 U and 10 U had significantly smaller LVDs than the control group. In addition, in groups with EPO 1 U and 10 U, FAC was significantly larger and AL was significantly smaller than in the control group and groups with EPO 0.1 U and 100 U.

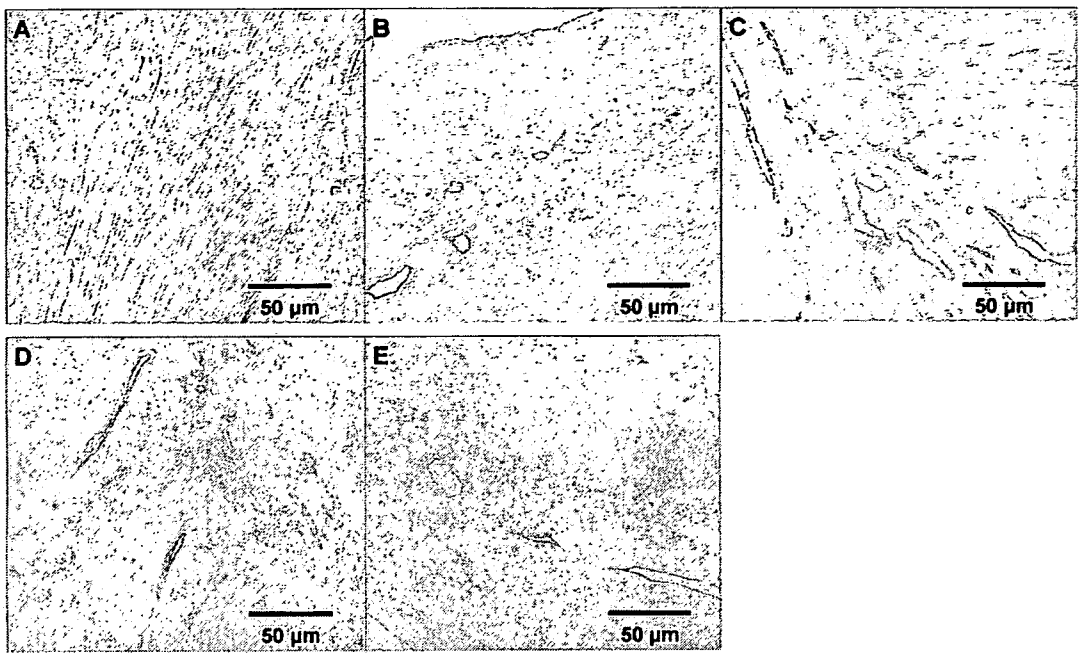

Fig 3. Immunohistochemistry for von Willebrand factor (brown, ×100). (A–E) representative images of the peri-MI area from control, erythropoietin 0.1 U, 1 U, 10 U, and 100 U groups, respectively.

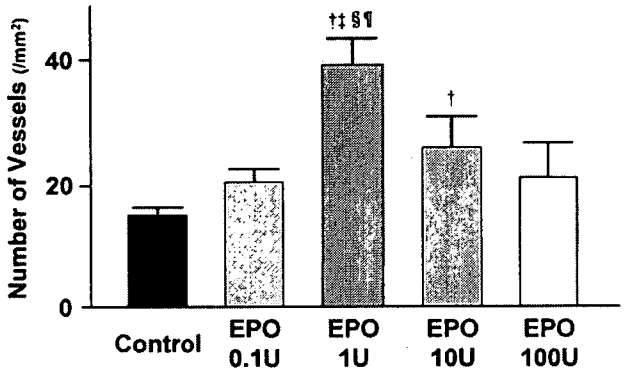

Fig 4. Vascular density in the peri-MI area. EPO, erythropoietin. †p<0.05 vs control, ‡p<0.05 vs EPO 0.1 U, §p<0.05 vs EPO 10 U, ¶p<0.05 vs EPO 100 U.

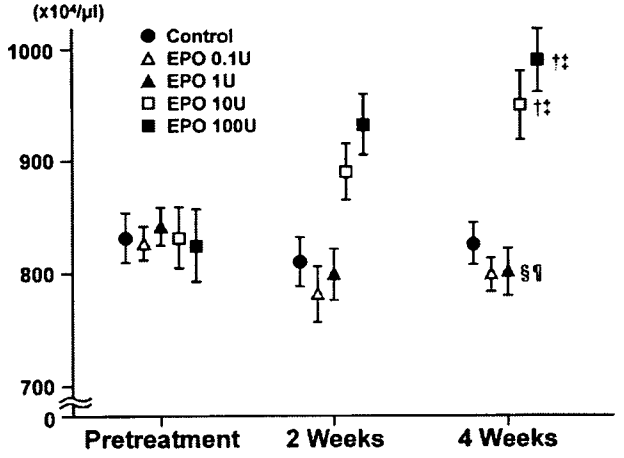

Fig 5. Red blood cell count. Error bars show SEM. EPO, erythropoietin. †p<0.05 vs control, ‡p<0.05 vs EPO 0.1 U, §p<0.05 vs EPO 10 U, ¶p<0.05 vs EPO 100 U.

Cardiac Catheterization

One-way factorial ANOVA showed a high group effect in both Ees and Tau (Fig 2). The Ees was the highest in the group with EPO 1 U (control: 0.12±0.01, EPO 0.1 U: 0.14±0.02, EPO 1 U: 0.33±0.08, EPO 10 U: 0.30±0.08, EPO 100 U: 0.15±0.02 mmHg/μl, respectively). Also, the Tau was the lowest in the group with EPO 1 U among them (control: 19.7±0.9, EPO 0.1 U: 19.3±1.0, EPO 1 U: 16.6±0.6, EPO 10 U: 16.9±0.8, EPO 100 U: 19.7±1.3 ms).

Vascular Density

Representative images are shown in Fig 3. The vascular density in the peri-MI area was highest in the group with EPO 1 U (control, EPO 0.1 U, 1 U, 10 U, 100 U: 13.68±2.49, 21.08±2.75, 37.97±4.19, 24.42±6.07, 21.54±4.68/mm², respectively). The vascular density in the group with EPO 10 U was significantly higher than in the control group (24.42±6.07 vs 13.68±2.49/mm²; p<0.05) (Fig 4).

RBC Analysis

In the groups with EPO 10 U and 100 U, the number of RBC at 4 weeks after treatment was significantly higher than in the control group. The number of RBC in the groups with EPO 0.1 U and 1 U was comparable with the control group (Fig 5) (control, EPO 0.1 U, 1 U, 10 U, 100 U; pretreatment baseline: 832±22, 827±15, 842±17, 832±27, 825±32×10⁴/μl; 4 weeks: 826±19, 798±15, 801±21, 949±30, 989±28×10⁴/μl).

Discussion

The salient findings of this study are as follows: (1) the SR system with EPO enabled release of EPO from a gelatin hydrogel sheet over a period greater than 3 weeks, and (2) the most relevant dose of EPO incorporated in the sheet for

improving LV function without inducing polycythemia was 1 U in the rat chronic MI model.

It is pertinent to comment on reasons why we used SR EPO sheets rather than gelatin hydrogel microspheres incorporating EPO. In our earlier studies, gelatin hydrogel microspheres[28–31] and sheets[6,7] were used as a carrier of SR bFGF. For the purpose of healing of devascularized sternum, we used gelatin sheets incorporating bFGF, for anatomical reasons[6,7] but in the case of MI, we injected a solution of 100 μl containing gelatin bFGF microspheres into several sites of the border zones of MI scar tissue.[28,29] There are several limitations to that therapeutic approach. First, intramyocardial injection itself may injure the myocardium. Second, the thin scar tissue may limit the appropriate space for microsphere retention. Finally, it is difficult to determine the local concentration of released bFGF in situ. Epicardial application of gelatin sheets may overcome these disadvantages and in fact, gelatin hydrogel sheets incorporating other angiographic growth factors are being used in experimental settings.[24,25] An epicardial application of a bone-marrow-cell-seeded biodegradable polymeric scaffold is reported to be useful for enhancing angiogenesis and improving myocardial function in the infarcted heart.[32]

It is tempting to speculate about how EPO suppresses LV remodeling and ameliorates LV contractility and relaxation after MI. There are 3 possible mechanisms responsible for the reduction of functional decline after MI (ie, progression in the LV observed in rats of the control group in the present study). First of all, augmented angiogenesis might contribute to functional recovery after MI. In the present study, the vascular density in the peri-MI area was positively correlated with FAC and Ees, and negatively correlated with AL and Tau. Although a good correlation does not necessarily indicate a cause–effect relationship, it is conceivable that EPO-induced angiogenesis might ameliorate LV functional recovery. Our speculation is supported by the fact that EPO accelerates naturally occurring capillary overgrowth as powerfully as vascular endothelial growth factor.[33] Second, favorable effects with EPO may result from its ability to reduce apoptotic cell death. It has been demonstrated that the number of apoptotic cardiomyocytes in the infarct area was decreased significantly by EPO treatment in a rat AMI model[14,15,19] although EPO administration did not affect the apoptosis of cardiomyocytes in a rat chronic MI model.[18] This discrepancy may be explained by the fact that apoptotic cell death tapers with the progression of pathological changes of MI.[34] In fact, in the present study reported here, approximately 0.1% nuclei of cardiomyocytes were TUNEL positive in the area at risk of untreated hearts at 8 weeks after coronary artery ligation. Thus, the contribution toward prevention of apoptosis by EPO treatment may be minimal, if any, in our experimental model. Another beneficial effect of EPO treatment may be its anti-inflammatory effects via attenuation of pro-inflammatory cytokine production.[35] However, it is difficult to specify these favorable effects to EPO, because prevention of LV remodeling by EPO treatment may result in subsidence of the inflammatory response to myocardial ischemic injury.

Previous investigators have attempted to find the optimal EPO dose for improving LV function without inducing polycythemia in the chronic MI model. van der Meer et al produced LV functional improvement with intraperitoneal EPO administration at a dose of 8,000 U/kg;[18] however, significant polycythemia inevitably occurred. In contrast, a single intravenous injection of 1,000 U/kg EPO did not improve LV function.[36] Thus, it is difficult to determine the therapeutically useful EPO dose in the chronic MI model. Our therapeutic approach with a SR drug delivery system overcame these problems of EPO treatment. Indeed, when a 1 U EPO gelatin sheet was applied, the plasma EPO concentration was augmented by less than 0.5%, which is negligible in comparison with the more than 100-fold increase in the case of a single intraperitoneal EPO injection at a dose of 8,000 U/kg.[18] Thus, the clinical application of EPO treatment for chronic MI is promising with the use of this newly developed drug delivery system.

It deserves some comment why the 100 U EPO did not improve the endpoints. As shown in Fig 2, myocardial function was most improved with 1 U EPO treatment, and it showed a gradual deterioration with increasing doses of EPO. The dose-independency may be, at least in part, explained by the fact that polycythemia associated with 10 U and 100 U EPO treatment may disturb the microcirculation in the infarcted area because of the high blood viscosity. Further studies are necessary to elucidate the paradoxical dose-dependency with EPO treatment.

Study Limitations

For gelatin hydrogel sheet application, re-opening the chest is inevitable at 4 weeks after AMI, which is more invasive than a single intravenous injection of EPO. The disadvantage may be counterbalanced by combined coronary artery bypass grafting surgery. Another limitation to the clinical application of the new treatment strategy is the relatively narrow window of optimal doses with EPO. To overcome these drawbacks, clinical studies are needed to determine the optimal dose of EPO in humans.

In future, we need to conduct double-blind, randomized controlled clinical trials to establish the effects of SR EPO treatment on surrogate markers such as LV ejection fraction, myocardial perfusion and exercise tolerance in patients with ungraftable viable myocardium.

In conclusion, application of gelatin hydrogel sheets incorporating 1 U EPO successfully reversed LV remodeling without inducing polycythemia in the rat chronic MI model. This new treatment strategy to treat ischemic cardiomyopathy will be realized in the clinical setting in the near future.

Acknowledgments

We would like to express our sincere gratitude to Mrs Fumiyo Kataoka for her expert technical assistance, and acknowledge the meticulous assistance of Miss Yukiko Okumura during the preparation of this manuscript.

References

1. Simons M, Annex BH, Laham RJ, Kleiman N, Henry T, Dauerman H, et al. Pharmacological treatment of coronary artery disease with recombinant fibroblast growth factor-2: Double-blind, randomized, controlled clinical trial. *Circulation* 2002; **105**: 788–793.
2. Henry TD, Annex BH, McKendall GR, Azrin MA, Lopez JJ, Giordano FJ, et al. The VIVA trial: Vascular endothelial growth factor in Ischemia for Vascular Angiogenesis. *Circulation* 2003; **107**: 1359–1365.
3. Laham RJ, Sellke FW, Edelman ER, Pearlman JD, Ware JA, Brown DL, et al. Local perivascular delivery of basic fibroblast growth factor in patients undergoing coronary bypass surgery: Results of a phase I randomized, double-blind, placebo-controlled trial. *Circulation* 1999; **100**: 1865–1871.
4. Losordo DW, Vale PR, Hendel RC, Milliken CE, Fortuin FD, Cummings N, et al. Phase 1/2 placebo-controlled, double-blind, dose-escalating trial of myocardial vascular endothelial growth factor 2 gene transfer by catheter delivery in patients with chronic myocardial ischemia. *Circulation* 2002; **105**: 2012–2018.
5. Grines CL, Watkins MW, Mahmarian JJ, Iskandrian AE, Rade JJ,

Marrott P, et al. A randomized, double-blind, placebo-controlled trial of Ad5FGF-4 gene therapy and its effect on myocardial perfusion in patients with stable angina. *J Am Coll Cardiol* 2003; **42:** 1339–1347.
6. Iwakura A, Tabata Y, Miyao M, Ozeki M, Tamura N, Ikai A, et al. Novel method to enhance sternal healing after harvesting bilateral internal thoracic arteries with use of basic fibroblast growth factor. *Circulation* 2000; **102**(Suppl III): III-307–III-311.
7. Iwakura A, Tabata Y, Tamura N, Doi K, Nishimura K, Nakamura T, et al. Gelatin sheet incorporating basic fibroblast growth factor enhances healing of devascularized sternum in diabetic rats. *Circulation* 2001; **104**(Suppl I): I-325–I-329.
8. Brines ML, Ghezzi P, Keenan S, Agnello D, de Lanerolle NC, Cerami C, et al. Erythropoietin crosses the blood–brain barrier to protect against experimental brain injury. *Proc Natl Acad Sci USA* 2000; **97:** 10526–10531.
9. Kaptanoglu E, Solaroglu I, Okutan O, Surucu HS, Akbiyik F, Beskonakli E. Erythropoietin exerts neuroprotection after acute spinal cord injury in rats: Effect on lipid peroxidation and early ultrastructural findings. *Neurosurg Rev* 2004; **27:** 113–120.
10. Junk AK, Mammis A, Savitz SI, Singh M, Roth S, Malhotra S, et al. Erythropoietin administration protects retinal neurons from acute ischemia-reperfusion injury. *Proc Natl Acad Sci USA* 2002; **99:** 10659–10664.
11. Grimm C, Wenzel A, Groszer M, Mayser H, Seeliger M, Samardzija M, et al. HIF-1-induced erythropoietin in the hypoxic retina protects against light-induced retinal degeneration. *Nat Med* 2002; **8:** 718–724.
12. Vesey DA, Cheung C, Pat B, Endre Z, Gobe G, Johnson DW. Erythropoietin protects against ischaemic acute renal injury. *Nephrol Dial Transpl* 2004; **19:** 348–355.
13. Calvillo L, Latini R, Kajstura J, Leri A, Anversa P, Ghezzi P, et al. Recombinant human erythropoietin protects the myocardium from ischemia-reperfusion injury and promotes beneficial remodeling. *Proc Natl Acad Sci USA* 2003; **100:** 4802–4806.
14. Moon C, Krawczyk M, Ahn D, Ahmet I, Paik D, Lakatta EG, et al. Erythropoietin reduces myocardial infarction and left ventricular functional decline after coronary artery ligation in rats. *Proc Natl Acad Sci USA* 2003; **100:** 11612–11617.
15. Parsa CJ, Matsumoto A, Kim J, Riel RU, Pascal LS, Walton GB, et al. A novel protective effect of erythropoietin in the infarcted heart. *J Clin Invest* 2003; **112:** 999–1007.
16. Parsa CJ, Kim J, Riel RU, Pascal LS, Thompson RB, Petrofski JA, et al. Cardioprotective effects of erythropoietin in the reperfused ischemic heart: A potential role for cardiac fibroblasts. *J Biol Chem* 2004; **279:** 20655–20662.
17. Cai Z, Manalo DJ, Wei G, Rodriguez ER, Fox-Talbot K, Lu H, et al. Hearts from rodents exposed to intermittent hypoxia or erythropoietin are protected against ischemia-reperfusion injury. *Circulation* 2003; **108:** 79–85.
18. van der Meer P, Lipsic E, Henning RH, Boddeus K, van der Velden J, Voors AA, et al. Erythropoietin induces neovascularization and improves cardiac function in rats with heart failure after myocardial infarction. *J Am Coll Cardiol* 2005; **46:** 125–133.
19. Moon C, Krawczyk M, Paik D, Coleman T, Brines M, Juhaszova M, et al. Erythropoietin, modified to not stimulate red blood cell production, retains its cardioprotective properties. *J Pharmacol Exp Ther* 2006; **316:** 999–1005.
20. Bullard AJ, Yellon DM. Chronic erythropoietin treatment limits infarct-size in the myocardium in vitro. *Cardiovasc Drug Ther* 2005; **19:** 333–336.
21. Tabata Y, Hijikata S, Ikada Y. Enhanced vascularization and tissue granulation by basic fibroblast growth factor impregnated in gelatin hydrogels. *J Control Release* 1994; **31:** 189–199.
22. Fukunaka Y, Iwanaga K, Morimoto K, Kakemi M, Tabata Y. Controlled release of plasmid DNA from cationized gelatin hydrogels based on hydrogel degradation. *J Control Release* 2002; **80:** 333–343.
23. Sakakibara Y, Nishimura K, Tambara K, Yamamoto M, Lu F, Tabata Y, et al. Prevascularization with gelatin microspheres containing basic fibroblast growth factor enhances the benefits of cardiomyocyte transplantation. *J Thorac Cardiovasc Surg* 2002; **124:** 50–56.
24. Sakaguchi G, Tambara K, Sakakibara Y, Ozeki M, Yamamoto M, Premaratne G, et al. Control-released hepatocyte growth factor prevents the progression of heart failure in stroke-prone spontaneously hypertensive rats. *Ann Thorac Surg* 2005; **79:** 1627–1634.
25. Tambara K, Premaratne GU, Sakaguchi G, Kanemitsu N, Lin X, Nakajima H, et al. Administration of control-released hepatocyte growth factor enhances the efficacy of skeletal myoblast transplantation in rat infarcted hearts by greatly increasing both quantity and quality of the graft. *Circulation* 2005; **112**(Suppl II): II-129–II-134.
26. Sakakibara Y, Tambara K, Lu F, Nishina T, Sakaguchi G, Nagaya N, et al. Combined procedure of surgical repair and cell transplantation for left ventricular aneurysm: An experimental study. *Circulation* 2002; **106**(Suppl I): I-193–I-197.
27. Tambara K, Sakakibara Y, Sakaguchi G, Lu F, Premaratne GU, Lin X, et al. Transplanted skeletal myoblasts can fully replace the infarcted myocardium when they survive in the host in large numbers. *Circulation* 2003; **108**(Suppl II): II-259–II-263.
28. Yamamoto T, Suto N, Okubo T, Mikuniya A, Hanada H, Yagihashi S, et al. Intramyocardial delivery of basic fibroblast growth factor-impregnated gelatin hydrogel microspheres enhances collateral circulation to infarcted canine myocardium. *Jpn Circ J* 2001; **65:** 439–444.
29. Iwakura A, Fujita M, Kataoka K, Tambara K, Sakakibara Y, Komeda M, et al. Intramyocardial sustained delivery of basic fibroblast growth factor improves angiogenesis and ventricular function in a rat infarct model. *Heart Vessels* 2003; **18:** 93–99.
30. Shao ZQ, Takaji K, Katayama Y, Kunitomo R, Sakaguchi H, Lai ZF, et al. Effects of intramyocardial administration of slow-release basic fibroblast growth factor on angiogenesis and ventricular remodeling in a rat infarct model. *Circ J* 2006; **70:** 471–477.
31. Hirose K, Fujita M, Marui A, Arai Y, Sakaguchi H, Huang Y, et al. Combined treatment of sustained-release basic fibroblast growth factor and sarpogrelate enhances collateral blood flow effectively in rabbit hindlimb ischemia. *Circ J* 2006; **70:** 1190–1194.
32. Fukuhara S, Tomita S, Nakatani T, Fujisato T, Ohtsu Y, Ishida M, et al. Bone marrow cell-seeded biodegradable polymeric scaffold enhances angiogenesis and improves function of the infracted heart. *Circ J* 2005; **69:** 850–857.
33. Jaquet K, Krause K, Tawakol-Khodai M, Geidel S, Kuck KH. Erythropoietin and VEGF exhibit equal angiogenic potential. *Microvasc Res* 2002; **64:** 326–333.
34. Palojoki E, Saraste A, Eriksson A, Pulkki K, Kallajoki M, Voipio-Pulkki LM, et al. Cardiomyocyte apoptosis and ventricular remodeling after myocardial infarction in rats. *Am J Physiol Heart Circ Physiol* 2001; **280:** 2726–2731.
35. Villa P, Bigini P, Mennini T, Agnello D, Laragione T, Cagnotto A, et al. Erythropoietin selectively attenuates cytokine production and inflammation in cerebral ischemia by targeting neuronal apoptosis. *J Exp Med* 2003; **198:** 971–975.
36. Hirata A, Minamino T, Asanuma H, Fujita M, Wakeno M, Myoishi M, et al. Erythropoietin enhances neovascularization of ischemic myocardium and improves left ventricular dysfunction after myocardial infarction in dogs. *J Am Coll Cardiol* 2006; **48:** 176–184.

Circ J 2007; **71:** 412–417

Combined Treatment With Sustained-Release Basic Fibroblast Growth Factor and Heparin Enhances Neovascularization in Hypercholesterolemic Mouse Hindlimb Ischemia

Yoshio Arai, MD; Masatoshi Fujita, MD*; Akira Marui, MD; Keiichi Hirose, MD; Hisashi Sakaguchi, MD; Tadashi Ikeda, MD; Yasuhiko Tabata, PhD**; Masashi Komeda, MD

Background Whether the combined treatment with sustained-release basic fibroblast growth factor (bFGF) and heparin enhances neovascularization in hypercholesterolemic mouse hindlimb ischemia was investigated.
Methods and Results Wild-type C57BL/6 and low density lipoprotein receptor-deficient mice were assigned to 1 of the following 4 experimental groups and treated for 2 weeks after femoral artery extraction: group N, no treatment; group H, daily subcutaneous injection of heparin calcium; group F, single intramuscular injection of the sustained-release bFGF microspheres; and group FH, combined treatment with sustained-release bFGF and heparin. Among the wild-type mice at 4 weeks after femoral artery extraction, the laser Doppler perfusion image index (LDPII) in groups H, F, and FH was significantly higher than that in group N. The vascular density in group FH was the highest among the 4 groups. The maturation index in the 3 treated groups was significantly higher than that in group N. Among the hypercholesterolemic mice, the LDPII in group FH was significantly higher than that in the other 3 groups. The vascular density and maturation index in group FH were the highest among the 4 groups.
Conclusions Combined treatment with sustained-release bFGF and heparin enhanced neovascularization in the hypercholesterolemic hindlimb ischemia model. (*Circ J* 2007; **71:** 412–417)

Key Words: Basic fibroblast growth factor; Heparin; Hindlimb ischemia; Hypercholesterolemia; Neovascularization

The use of targeted stimulation of neovascularization as a therapeutic tool for restoring blood flow to an ischemic limb that is affected by peripheral arterial disease has been challenged for the past decade. Typically, therapeutic neovascularization is performed by the local delivery of angiogenic growth factor genes or proteins to the ischemic limb. However, concerns regarding the unpredictable duration and level of gene expression as well as responses of genetic materials persist! Because angiogenic growth factors have a rapid clearance rate, their efficacy is limited? To overcome this drawback, controlled forms of these growth factors have been developed for their sustained release?[3–5] We and others have recently demonstrated the effectiveness of gelatin hydrogel microspheres incorporating basic fibroblast growth factor (bFGF) for the treatment of various pathological conditions including hindlimb ischemia?[6–11] However, it has been noted that a single use of sustained-release bFGF is insufficient for a complete revascularization. Therefore, we have proposed combination strategies with hepatocyte growth factor[9] and sarpogrelate![10]

Heparin treatment has been reported to accelerate neovascularization in a variety of experimental models including those of hindlimb ischemia![12–15] Although the precise beneficial mechanisms of heparin treatment have not been completely clarified, the interaction of heparin, endogenous bFGF![16–19] and hepatocyte growth factor[20,21] has been proposed.

Accordingly, in the present study, we have attempted, for the first time, the simultaneous administration of sustained-release bFGF and heparin in the hindlimb ischemia model. To further clarify the effectiveness of combined treatment with sustained-release bFGF and heparin, we utilized hypercholesterolemic mice with an impaired angiogenic response to the ischemic stimulus?[22,23]

Thus, we evaluated a new combined treatment with sustained-release bFGF and heparin in the hypercholesterolemic mouse hindlimb ischemia model.

Methods

Animal Preparations

Six-week-old male wild-type C57BL/6 mice were purchased from Japan SLC (Shizuoka, Japan). Six-week-old male low-density lipoprotein receptor-knockout mice (LDLR -/- mice; C57BL/6 background) were purchased from the Jackson Laboratory (Bar Harbor, ME, USA). For

(Received October 20, 2006; revised manuscript received December 7, 2006; accepted December 21, 2006)
*Department of Cardiovascular Surgery, Kyoto University Graduate School of Medicine, *School of Health Sciences, Faculty of Medicine and **Department of Biomaterials, Institute for Frontier Medical Sciences, Kyoto University, Kyoto, Japan*
Mailing address: Masatoshi Fujita, MD, School of Health Sciences, Faculty of Medicine, Kyoto University, 53 Kawahara-cho, Shogoin, Sakyo-ku, Kyoto 606-8507, Japan. E-mail: mfujita@kuhp.kyoto-u.ac.jp

Table 1 Lipids and BW Profiles in Wild-Type and LDLR -/- Mice

Groups·Age	6 weeks	8 weeks	10 weeks	14 weeks	18 weeks	22 weeks
Wild-type (n=12)						
TC (mg/dl)	70±17	67±14	51±7	50±14	51±10	59±10
TG (mg/dl)	50±14	59±17	63±24	53±17	44±21	54±14
BW (g)	26.0±1.0	26.6±1.0	26.7±1.7	27.9±0.6	28.3±2.1†	29.5±3.1†
LDLR -/- mice (n=12)						
TC (mg/dl)	134±28*	519±59*,†	1,223±135*,†	1,416±236*,†	1,320±166*,†	1,471±290*,†
TG (mg/dl)	96±17*	209±48*,†	348±83*,†	390±76*,†	359±66*,†	324±87*,†
BW (g)	27.0±1.7	27.5±2.1	30.0±1.7*	30.6±2.4*,†	32.0±2.4*,†	33.1±3.1*,†

Data are mean ± standard deviation.
**p<0.05 vs wild-type, †p<0.05 vs values at 6 weeks.*
BW, body weight; LDLR -/- mice, low-density lipoprotein receptor-knockout mice; TC, total cholesterol; TG, triglyceride.

4 months, 12 wild-type mice were fed a normal mouse diet (Oriental Yeast Co, Chiba, Japan) containing <0.04% cholesterol and 4% fat. For 4 months, 12 LDLR -/- mice were fed a high-fat diet (Oriental Yeast Co, Chiba, Japan) containing 1.25% cholesterol and 15.1% fat, as described previously[22,23]

Lipoprotein Profile and Body Weight Analysis

Plasma total cholesterol (TC) and triglyceride (TG) levels were determined at 2 to 4-week intervals by using an enzymatic colorimetric assay method (TC: Cholescolor liquid; TG: Lipids liquid; TOYOBO, Osaka, Japan). Blood samples for these assays were obtained from the retro-orbital plexus of the 24 anesthetized mice and were collected in heparinized tubes. Body weight, TC, and TG were simultaneously measured.

The Kyoto University Animal Experiment Committee approved the experiment protocol. The animals were cared for in compliance with the Guidelines for the Care and Use of Laboratory Animals published by USA National Institutes of Health (NIH Publication No. 85-23, revised 1996).

Preparation of Gelatin Hydrogel Microspheres Containing bFGF

Gelatin hydrogel microspheres containing bFGF were prepared as described previously[6-10] Gelatin microspheres were prepared by crosslinking glutaraldehyde of gelatin in the dispersed state[3,4] The average diameter of the freeze-dried microspheres was 26μm. When calculated from their volume before and after swelling in phosphate-buffered saline (PBS) solution for 24 h at 37°C, the water content of the gelatin microspheres was 95 wt%. Human recombinant bFGF was incorporated into the gelatin microspheres by dropping 26μm of bFGF in solution (20μl) into 2 mg of freeze-dried gelatin microspheres; the microspheres were then left at room temperature for 3 h. At use, the bFGF-containing gelatin hydrogel microspheres were dispersed in 100μl PBS, aspirated into a 1-ml syringe attached with a 27-gauge needle (Terumo, Tokyo, Japan), and injected into the 5 sites of ischemic thigh muscles of mice hindlimb.

Experimental Design

Hindlimb ischemia was created in 18-week-old male wild-type and LDLR -/- mice. Briefly, after the mice were anesthetized by an intraperitoneal sodium pentobarbital (60 mg/kg) injection, the right groin area was shaved and prepped with povidone-iodine. The entire right saphenous artery and vein, right external iliac artery and vein, and deep femoral and circumflex arteries and veins were ligated, cut, and excised to obtain a murine model of severe hindlimb ischemia as described previously[9]

Eighty wild-type and LDLR -/- mice were randomly assigned to 4 groups (n=10 per group) depending on the treatment arms: no treatment (group N), daily subcutaneous injection of 10 U heparin calcium (1,000 U/ml; Caprocin; Sawai Pharm Co, Osaka, Japan) in 0.1 ml PBS solution at the back of mice for 14 days from the second day after femoral artery extraction (group H), treatment with microspheres containing 10μg bFGF injected into 5 sites in the thigh muscles of the ischemic hindlimb by using a 27-gauge needle 2 days after femoral artery extraction (group F), and combined treatment of sustained-release bFGF and heparin in the same manner as that for groups F and H (group FH).

At 4 weeks after the initiation of treatment, the animals were re-anesthetized by an intraperitoneal injection of pentobarbital (60 mg/kg), subjected to the measurements described below, and then sacrificed with an overdose of pentobarbital for histological examination.

Hindlimb Blood Perfusion

Hindlimb blood perfusion was scanned by using a laser Doppler perfusion image (LDPI) analyzer (Moor Instruments, Devon, UK) on the first day of treatment (2 days after surgery) and then every 7 days. To eliminate the influence of the surgical procedure, the average blood perfusion of the bilateral feet was evaluated. To minimize influential variables including ambient light and temperature, perfusion was expressed as the ratio of the blood perfusion in the right (ischemic) limb to that in the left (non-ischemic) limb of the same mouse, that is, in terms of the LDPI index (LDPII)[9,24]

Immunohistological Analysis

Four weeks after the initiation of treatment, the mice were euthanized and perfusion-fixed with 4% paraformaldehyde. The ischemic calf muscles were embedded in optimal cutting temperature compound (Sakura Finetechnical, Tokyo, Japan) and frozen at −80°C. Cryostat sections (5-μm thick) of the tissues were stained with rabbit polyclonal anti-human von Willebrand factor antibody (vWF; Dako Japan, Kyoto, Japan) or mouse monoclonal anti-human smooth muscle actin antibody (SMA; Sigma-Aldrich Japan K.K., Tokyo, Japan). As the negative control, rabbit normal immunoglobulin fraction (Dako Japan, Kyoto, Japan) was used to show antibody specificity. From each mouse, 8 random fields on 2 different sections (approximately 3 mm apart) were photographed with a digital camera (Olympus, Tokyo, Japan). The number of vWF (endothelial marker)-positive (capillaries and arterioles) or SMA (vascular smooth muscle marker)-positive vessels (arterioles) was counted manually

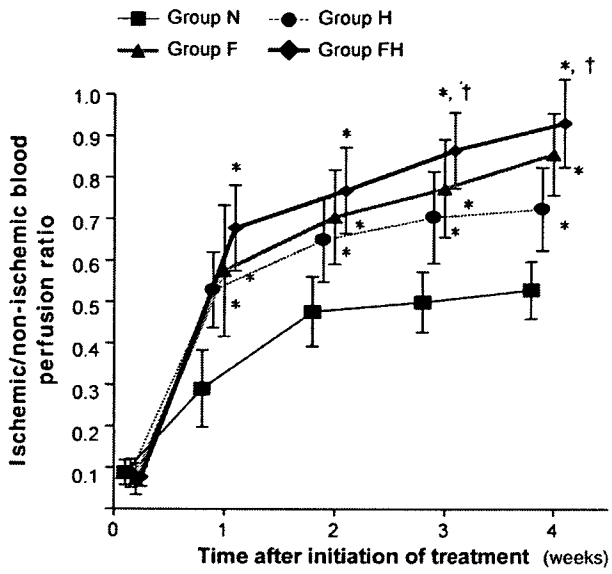

Fig 1. Time-course of ischemic/non-ischemic blood perfusion ratio in wild-type mice after treatment. Group F, treatment with sustained-release basic fibrobloast growth factor (bFGF); group FH, combined treatment with sustained-release bFGF and heparin; group H, treatment with heparin; group N, no treatment. *p<0.05 vs group N. †p<0.05 vs group H.

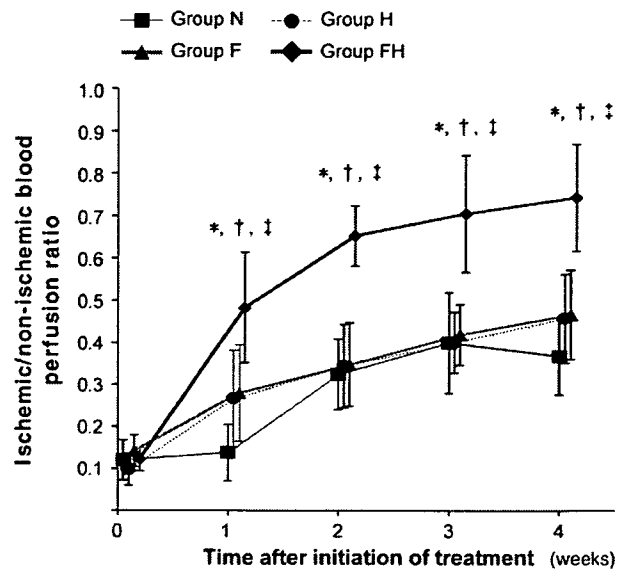

Fig 2. Time-course of ischemic/non-ischemic blood perfusion ratio in hypercholesterolemic mice after treatment. Group F, treatment with sustained-release basic fibrobloast growth factor (bFGF); group FH, combined treatment with sustained-release bFGF and heparin; group H, treatment with heparin; group N, no treatment. *p<0.05 vs group N. †p<0.05 vs group H. ‡p<0.05 vs group F.

in a blind fashion. Vascular density was calculated by counting the number of vWF-positive vessels. The maturation index was determined as the ratio of the percentage of SMA-positive vessels to that of vWF-positive vessels[9]

Statistical Analysis

Results were expressed as the mean±standard deviation. Differences among groups were determined by 1-way analysis of variance followed by multiple comparisons using the Bonferroni/Dunn's test. All statistical analyses were performed by using the StatviewTM software (Abacus, MI, USA). A p value <0.05 was considered significant.

Results

None of the mice died because of the surgical manipulation. We found no complications attributable to the topical use of the sustained-release bFGF and heparin injection.

Lipids and Body Weight Profiles

The plasma TC and TG levels in the LDLR -/- mice were remarkably increased 2 weeks after they were fed a high-fat chow, while those in wild-type mice fed with normal chow remained unchanged. The body weight of both wild-type and hypercholesterolemic mice increased gradually. The body weight of hypercholesterolemic mice was significantly higher than that of the wild-type mice 4 weeks after feeding (Table 1).

Hindlimb Blood Perfusion

The time course of LDPII in the wild-type and hypercholesterolemic mice are depicted in Figs 1,2. Among the wild-type mice, the LDPII in groups H, F and FH was higher than that in the control group 4 weeks after treatment (53±7%, 73±10%, 86±10%, and 93±11% for groups N, H, F, and FH, respectively; p<0.05). The LDPII in group FH was significantly higher than that in group H. No statistically significant difference in the LDPII was observed between groups F and FH (Fig 1). The LDPII in the untreated LDLR -/- mice was 39±9%, being significantly (p<0.05) lower than 53±7% in the untreated wild-type mice. Among the hypercholesterolemic mice, the LDPII in group FH was higher than those in the other 3 groups 4 weeks after treatment (39±9%, 46±11%, 47±10%, and 74±13% for groups N, H, F, and FH, respectively; p<0.05). No statistically significant difference in the LDPII was observed among groups N, H, and F (Fig 2).

Vascular Density

Representative photomicrographs of histological sections from the wild-type and hypercholesterolemic mice are shown in Fig 3A. Among the wild-type mice, the vascular density in groups H, F, and FH was significantly higher than that in the control group (189±46, 263±46, 318±31, and 383±59 vessels/mm^2 for groups N, H, F, and FH, respectively; p<0.05). The vascular density in group FH was the highest among the 4 groups (Fig 3B). Among the hypercholesterolemic mice, the vascular density in group FH was significantly higher than those in the other 3 groups (120±25, 116±32, 131±27, and 282±48 vessels/mm^2 for groups N, H, F, and FH, respectively; p<0.01). No statistically significant difference in the vascular density was observed between groups N, H, and F (Fig 3B).

Vascular Maturity

Representative photomicrographs of histological sections from the wild-type and hypercholesterolemic mice are shown in Fig 4A. Among the wild-type mice, the percentage of mature vessels in groups H, F, and FH was significantly higher than that in the control group (7±3%, 15±7%, 17±4%, and 19±6% for groups N, H, F, and FH, respectively; p<0.05). No statistically significant difference in the maturation index was observed between groups H, F, and FH (Fig 4B). Among the hypercholesterolemic mice, the

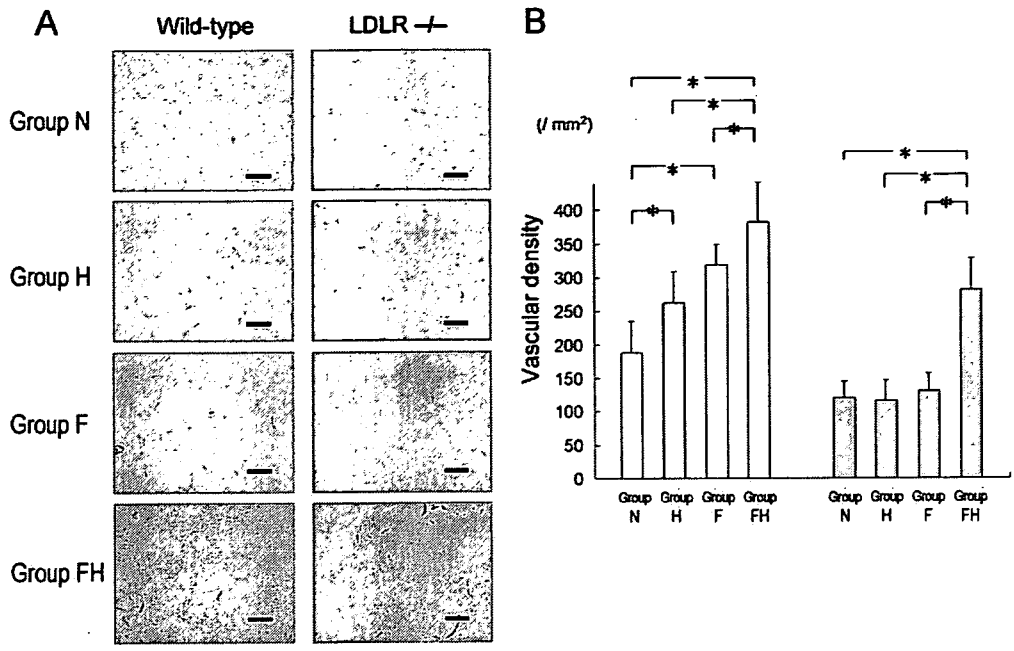

Fig 3. (A) Representative photomicrographs of ischemic calf muscles stained with anti-human von Willebrand factor antibody 4 weeks after femoral artery extraction. Scale bars indicate 100 μm. (B) Vascular density in the ischemic calf muscles of wild-type mice (open bar) and hypercholesterolemic mice (closed bar) 4 weeks after femoral artery extraction. Group F, treatment with sustained-release basic fibrobloast growth factor (bFGF); group FH, combined treatment with sustained-release bFGF and heparin; group H, treatment with heparin; group N, no treatment. *p<0.05. LDLR -/-, low-density lipoprotein receptor-knockout.

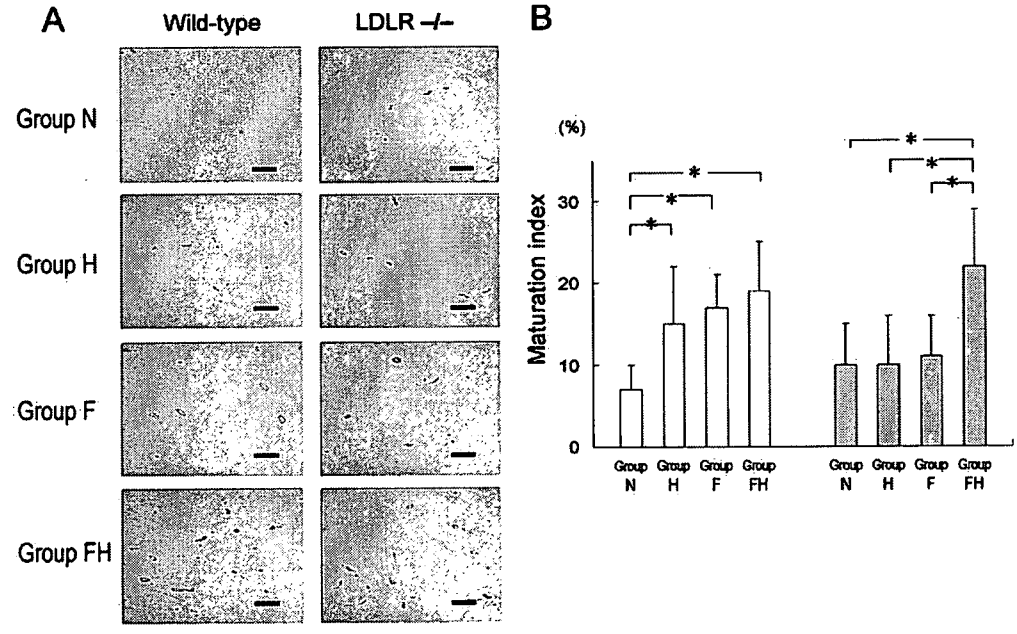

Fig 4. (A) Representative photomicrographs of ischemic calf muscles stained with anti-human smooth muscle actin antibody 4 weeks after femoral artery extraction; adjacent sections to Fig 3. Scale bars indicate 100 μm. (B) Vascular maturation index in the ischemic calf muscles of wild-type mice (open bar) and hypercholesterolemic mice (closed bar) 4 weeks after femoral artery extraction. Group F, treatment with sustained-release basic fibrobloast growth factor (bFGF); group FH, combined treatment with sustained-release bFGF and heparin; group H, treatment with heparin; group N, no treatment. *p<0.05. LDLR -/-, low-density lipoprotein receptor-knockout.

percentage of mature vessels in group FH was the highest among the 4 groups (10±5%, 10±6%, 11±5%, and 22±7% for groups N, H, F, and FH, respectively; p<0.01). No statistically significant difference in the maturation index was observed between groups N, H, and F (Fig 4B).

Discussion

The present study demonstrated the efficacy of the simultaneous administration of sustained-release bFGF and heparin on the restoration of collateral blood flow in the

hindlimb ischemia of hypercholesterolemic mice. To the best of our knowledge, this study is the first to show the effectiveness of a combined treatment with sustained-release bFGF and heparin on neovascularization in hindlimb ischemia. Our results would shed new light on the treatment of peripheral arterial disease.

To elucidate the efficacy of the combined therapy, we used LDLR -/- mice that had hypercholesterolemia because of reduced low-density lipoprotein (LDL) receptor expression. These animals develop increased plasma levels of total (predominantly LDL) cholesterol and a pattern of atherosclerosis that is similar to that observed in familial hypercholesterolemia. Hypercholesterolemia impairs collateral vessel growth, which was the case in the present study. However, it appears to be difficult to determine whether the impaired collateral vessel growth under hypercholesterolemia is caused by delayed native angiogenesis or a decreased magnitude of collateral vessel growth[25] because the extent of collateralization was evaluated only at 4 weeks after femoral artery extraction. A possible reason for the impaired neovascularization in hypercholesterolemia is that electronegative LDL downregulates bFGF via both transcriptional and posttranscriptional mechanisms[26,27] However, despite a suppressed availability of endogenous bFGF, hypercholesterolemic rabbits respond to exogenous bFGF[28] Another possible cause of impaired angiogenesis under hypercholesterolemia is the reduced nitric oxide bioactivity presumably because of reactive oxygen species production[29] It has been demonstrated that treatment of hypercholesterolemic rabbits with vascular endothelial growth factor improves collateral development[30] This might be explained by the fact that vascular endothelial growth factor augments nitric oxide release from vascular endothelium[31] However, the in vivo impact of hypercholesterolemia on collateral vessel development remains unclarified.

Based on the results of a preliminary study that involved the use of a variety of bFGF doses ranging from 5 to 40μg, we used gelatin hydrogel microspheres containing 10μg bFGF in the present study. In the normal non-treated mice, the LDPII was 51±8% at 4 weeks after femoral artery extraction. It increased to 86±12% by treatment with 10μg bFGF incorporated in gelatin hydrogel microspheres. Conversely, in the hypercholesterolemic mice, the LDPII at 4 weeks after surgery was low, that is, 36±10%. Treatment with 10, 20 and 40μg sustained-release bFGF increased it dose dependently to 47±11%, 58±21% and 88±10%, respectively. Based on these findings, we selected 10μg bFGF because this dose appeared to be suitable for the evaluation of the combined treatment with sustained-release bFGF and heparin, particularly in the case of hypercholesterolemic mice.

Neovascularization involves the proliferation of capillaries in the ischemic area (angiogenesis), new vessel formation by homing of endothelial progenitor cells (vasculogenesis), and maturation of preexisting collateral vessels (arteriogenesis); the last process is the most important in terms of increasing collateral blood flow[32] In the present study, we used the vascular maturation index instead of the angiographic approach to evaluate arteriogenesis. This is because mice are too small to be angiographically evaluated. Furthermore, in the present study, we used LDPII instead of microspheres to evaluate regional blood flow. This is also because mice are too small for their regional blood flow measurement with microspheres. Thus, we inferred that a larger-sized experimental animal appears necessary for the precise evaluation of arteriogenesis.

In the mice treated with heparin alone, neovascularization was significantly higher than that in the control mice, although heparin itself does not possess any angiogenic properties[33] In fact, the vascular density and maturation in the contralateral non-ischemic hindlimb in the heparin-treated mice were comparable with those in the control mice (data not shown). Because ischemia caused by femoral arterial extraction induces the production and release of bFGF, vascular growth factor and platelet-derived growth factor[34,35] it is likely that heparin potentiates the angiogenic effects of these endogenous growth factors[16–21,36,37]

Because the half-life of intravenously administrated heparin is short, that is, 90 min, in the present study, we used heparin calcium that has a longer half-life[33] The dose of heparin calcium used in the present study was approximately 400 U/kg, which was determined based on the data of previous studies (250–300 U/kg for rats[14] 300 U/kg for humans[33]). The dose-dependent effect of heparin was not evaluated in the present study. Therefore, future studies are required to elucidate the dose of heparin that is most appropriate for neovascularization, while also being cautious about the hemorrhagic and thrombocytopenic side effects of heparin.

In the present study, the beneficial effect of a combination treatment was exaggerated in the LDLR -/- mice. In the wild-type mice, both angiogenesis and arteriogenesis were augmented and almost saturated by a single treatment with sustained-release bFGF or heparin. In contrast, either single treatment was not so effective in the LDLR -/- mice (Figs 3,4). This may be because of blunt responses to the exogeneous bFGF and heparin in these mice. As a result, the combination treatment might have caused a remarkable difference in collateral development in the hypercholesterolemic mice.

In conclusion, combined treatment with sustained-release bFGF and heparin synergistically enhances neovascularization in the hindlimb ischemia of hypercholesterolemic mice with impaired angiogenic responses to the ischemic stimulus.

Acknowledgments

The authors thank Dr Shyamal Chandra Bir, Dr Yuang Huang (Kyoto University Graduate School of Medicine), Mrs Shiho Yuzawa and Mrs Yu Takeuchi (Suzuka University of Medical Science) for experimental assistance. This work was partially supported by a Grant for Scientific Research (No.16390395) from the Japanese Ministry of Education, Culture, Sports, Science and Technology.

References

1. Collinson DJ, Donnelly R. Therapeutic angiogenesis in peripheral arterial disease: Can biotechnology produce an effective collateral circulation? *Eur J Vasc Endovasc Surg* 2004; **28:** 9–23.
2. Baffour R, Berman J, Garb JL, Rhee SW, Kaufman J, Friedmann P. Enhanced angiogenesis and growth of collaterals by in vivo administration of recombinant basic fibroblast growth factor in a rabbit model of acute lower limb ischemia: Dose-response effect of basic fibroblast growth factor. *J Vasc Surg* 1992; **16:** 181–191.
3. Tabata Y, Ikada Y. Protein release from gelatin matrices. *Adv Drug Deli Rev* 1998; **31:** 287–301.
4. Tabata Y. Tissue regeneration based on growth factor release. *Tissue Eng* 2003; **9(Suppl 1):** S5–S15.
5. Edelman ER, Mathiowitz E, Langer R, Klagsbrun M. Controlled and modulated release of basic fibroblast growth factor. *Biomaterials* 1991; **12:** 619–626.
6. Yamamoto T, Suto N, Okubo T, Mikuniya A, Hanada H, Yagihashi S, et al. Intramyocardial delivery of basic fibroblast growth factor-impregnated gelatin hydrogel microspheres enhances collateral circula-

tion to infarcted canine myocardium. *Jpn Circ J* 2001; **65:** 439–444.
7. Iwakura A, Fujita M, Kataoka K, Tambara K, Sakakibara Y, Komeda M, et al. Intramyocardial sustained delivery of basic fibroblast growth factor improves angiogenesis and ventricular function in a rat infarct model. *Heart Vessels* 2003; **18:** 93–99.
8. Ueyama K, Bing G, Tabata Y, Ozeki M, Doi K, Nishimura K, et al. Development of biologic coronary artery bypass grafting in a rabbit model: Revival of a classic concept with modern biotechnology. *J Thorac Cardiovasc Surg* 2004; **127:** 1608–1615.
9. Marui A, Kanematsu A, Yamahara K, Doi K, Kushibiki T, Yamamoto M, et al. Simultaneous application of basic fibroblast growth factor and hepatocyte growth factor to enhance the blood vessels formation. *J Vasc Surg* 2005; **41:** 82–90.
10. Hirose K, Fujita M, Marui A, Arai Y, Sakaguchi H, Huang Y, et al. Combined treatment of sustained-release basic fibroblast growth factor and sarpogrelate enhances collateral blood flow effectively in rabbit hindlimb ischemia. *Circ J* 2006; **70:** 1190–1194.
11. Shao ZQ, Takaji K, Katayama Y, Kunitomo R, Sakaguchi H, Lai ZF, et al. Effects of intramyocardial administration of slow-release basic fibroblast growth factor on angiogenesis and ventricular remodeling in a rat infarct model. *Circ J* 2006; **70:** 471–477.
12. Fujita M. Heparin and angiogenic therapy. *Eur Heart J* 2000; **21:** 270–274.
13. Unger EF, Sheffield CD, Epstein SE. Heparin promotes the formation of extracardiac to coronary anastomoses in a canine model. *Am J Physiol Heart Circ Physiol* 1991; **260:** H1625–H1634.
14. Yang HT, Ogilvie RW, Terjung RL. Heparin increases exercise-induced collateral blood flow in rats with femoral artery ligation. *Circ Res* 1995; **76:** 448–456.
15. Carroll SM, White FC, Roth DM, Bloor CM. Heparin accelerates coronary collateral development in a porcine model of coronary artery occlusion. *Circulation* 1993; **88:** 198–207.
16. Schlessinger J, Plotnikov AN, Ibrahimi OA, Eliseenkova AV, Yeh BK, Yayon A, et al. Crystal structure of a ternary FGF-FGFR-heparin complex reveals a dual role for heparin in FGFR binding and dimerization. *Mol Cell* 2000; **6:** 743–750.
17. Ibrahimi OA, Yeh BK, Eliseenkova AV, Zhang F, Olsen SK, Igarashi M, et al. Analysis of mutations in fibroblast growth factor (FGF) and a pathogenic mutation in FGF receptor (FGFR) provides direct evidence for the symmetric two-end model for FGFR dimerization. *Mol Cell Biol* 2005; **25:** 671–684.
18. Chu CL, Goerges AL, Nugent MA. Identification of common and specific growth factor binding sites in heparan sulfate proteoglycans. *Biochemistry* 2005; **44:** 12203–12213.
19. Hung KW, Kumar TK, Kathir KM, Xu P, Ni F, Ji HH, et al. Solution structure of the ligand binding domain of the fibroblast growth factor receptor: Role of heparin in the activation of the receptor. *Biochemistry* 2005; **44:** 15787–15798.
20. Matsumori A, Ono K, Okada M, Miyamoto T, Sato Y, Sasayama S. Immediate increase in circulating hepatocyte growth factor/scatter factor by heparin. *J Mol Cell Cardiol* 1998; **30:** 2145–2149.
21. Maejima Y, Yasu T, Ueba H, Kobayashi N, Hashimoto S, Kubo N, et al. Exercise after heparin administration: New therapeutic program for patients with option arteriosclerosis obliterans. *Circ J* 2005; **69:** 1099–1104.
22. Tangirala RK, Rubin EM, Palinski W. Quantitation of atherosclerosis in murine models: Correlation between lesions in the aortic origin and in the entire aorta, and differences in the extent of lesions between sexes in LDL receptor-deficient and apolipoprotein E-deficient mice. *J Lipid Res* 1995; **36:** 2320–2328.
23. Ishibashi S, Brown MS, Goldstein JL, Gerard RD, Hammer RE, Herz J. Hypercholesterolemia in low density lipoprotein receptor knockout mice and its reversal by adenovirus-mediated gene delivery. *J Clin Invest* 1993; **92:** 883–893.
24. Couffinhal T, Silver M, Zheng LP, Kearney M, Witzenbichler B, Isner JM. Mouse model of angiogenesis. *Am J Pathol* 1998; **152:** 1667–1679.
25. Tirziu D, Moodie KL, Zhuang ZW, Singer K, Helisch A, Dunn JF, et al. Delayed arteriogenesis in hypercholesterolemic mice. *Circulation* 2005; **112:** 2501–2509.
26. Chen C-H, Jiang W, Via DP, Luo S, Li T-R, Lee Y-T, et al. Oxidized low-density lipoproteins inhibit endothelial cell proliferation by suppressing basic fibroblast growth factor expression. *Circulation* 2000; **101:** 171–177.
27. Chen C-H, Jiang T, Yang J-H, Jiang W, Lu J, Marathe GK, et al. Low-density lipoprotein in hypercholesterolemic human plasma induces vascular endothelial cell apoptosis by inhibiting fibroblast growth factor 2 transcription. *Circulation* 2003; **107:** 2102–2108.
28. Chen C-H, Cartwright J Jr, Li Z, Lou S, Nguyen HH, Gotto AM Jr, et al. Inhibitory effects of hypercholesterolemia and ox-LDL on angiogenesis-like endothelial growth in rabbit aortic explants. *Arterioscler Thromb Vasc Biol* 1997; **17:** 1303–1312.
29. Duan J, Murohara T, Ikeda H, Katoh A, Shintani S, Sasaki K, et al. Hypercholesterolemia inhibits angiogenesis in response to hindlimb ischemia: Nitric oxide-dependent mechanism. *Circulation* 2000; **102:** 370–376.
30. van Belle E, Rivard A, Chen D, Silver M, Bunting S, Ferrara N, et al. Hypercholesterolemia attenuates angiogenesis but does not preclude augmentation by angiogenic cytokines. *Circulation* 1997; **96:** 2667–2674.
31. van der Zee R, Murohara T, Luo Z, Zollmann F, Passeri J, Lekutat C, et al. Vascular endothelial growth factor/vascular permeability factor augments nitric oxide release from quiescent rabbit and human vascular endothelium. *Circulation* 1997; **95:** 1030–1037.
32. Schaper W, Scholz D. Factors regulating arteriogenesis. *Arterioscler Thromb Vasc Biol* 2003; **23:** 1143–1151.
33. Fujita M, Yamanishi K, Hirai T, Ohno A, Miwa K, Sasayama S. Comparative effect of heparin treatment with and without strenuous exercise on treadmill capacity in patients with stable effort angina. *Am Heart J* 1991; **122:** 453–457.
34. Luo F, Wariaro D, Lundberg G, Blegen H, Wahlberg E. Vascular growth factor expression in a rat model of severe limb ischemia. *J Surg Res* 2002; **108:** 258–267.
35. Faller DV. Endothelial cell responses to hypoxic stress. *Clin Exp Pharmacol Physiol* 1999; **26:** 74–84.
36. Jakobsson L, Kreuger J, Holmborn K, Lundin L, Eriksson I, Kjellen L, et al. Heparan sulfate in trans potentiates VEGFR-mediated angiogenesis. *Dev Cell* 2006; **10:** 625–634.
37. Rolny C, Spillmann D, Lindahl U, Claesson-Welsh L. Heparin amplifies platelet-derived growth factor (PDGF)-BB-induced PDGF alpha-receptor but not PDGF beta-receptor tyrosine phosphorylation in heparan sulfate-deficient cells: Effects on signal transduction and biological responses. *J Biol Chem* 2002; **277:** 19315–19321.